

# Metastable dynamical patterns and their stabilization in arrays of bidirectionally coupled sigmoidal neurons

Yo Horikawa\*

*Faculty of Engineering, Kagawa University, Takamatsu, 761-0396, Japan*

(Received 7 December 2012; revised manuscript received 5 September 2013; published 2 December 2013)

Transient patterns in a bistable ring of bidirectionally coupled sigmoidal neurons were studied. When the system had a pair of spatially uniform steady solutions, the instability of unstable spatially nonuniform steady solutions decreased exponentially with the number of neurons because of the symmetry of the system. As a result, transient spatially nonuniform patterns showed dynamical metastability: Their duration increased exponentially with the number of neurons and the duration of randomly generated patterns obeyed a power-law distribution. However, these metastable dynamical patterns were easily stabilized in the presence of small variations in coupling strength. Metastable rotating waves and their pinning in the presence of asymmetry in the direction of coupling and the disappearance of metastable dynamical patterns due to asymmetry in the output function of a neuron were also examined. Further, in a two-dimensional array of neurons with nearest-neighbor coupling, intrinsically one-dimensional patterns were dominant in transients, and self-excitation in these neurons affected the metastable dynamical patterns.

DOI: [10.1103/PhysRevE.88.062902](https://doi.org/10.1103/PhysRevE.88.062902)

PACS number(s): 05.45.-a, 87.19.lj

## I. INTRODUCTION

In spatially extended or coupled symmetric bistable systems, there exist metastable dynamical patterns, the duration (lifetimes) of which increases exponentially with system size or the number of elements. These are transient patterns and systems eventually reach asymptotically stable states, but the asymptotic states are never realized within a practical time when the systems are large. In other words, spatiotemporal patterns that remain for a long time and have been regarded as stable can collapse and disappear suddenly. These metastable dynamical patterns have been found in a one-dimensional bistable reaction-diffusion equation (the time-dependent Ginzburg-Landau equation, also called the Allen-Cahn equation) for phase transition [1]. A kinematical equation for the motion of kinks and antikinks has been derived, and it has been shown that the strength of attractive interaction between kinks and antikinks decreases exponentially with the distance between them. Their motion is exponentially slow when the distance is large, so it takes an extremely long time until they collide and disappear. Such metastable dynamical patterns have been shown in multidimensional domains and several spatially extended systems [2]. Further, it has been shown that metastable dynamics remains in a spatially discrete bistable reaction-diffusion equation when the distance between a kink and an antikink is large [3]. However, metastable dynamical patterns are pinned so stable spatially nonuniform steady solutions are generated due to discretization when a diffusion coefficient is small [4].

Transient dynamics in nervous systems and neural networks have also attracted much attention [5]. Some neural information processing is considered to be carried out by transient spatiotemporal patterns, not asymptotically stable states. This is because asymptotically stable states may not be realized within a short response time in actual nervous

systems. The responses of sensory systems to stimuli may consist of transitions among multiple stable states of neuronal assemblies. It has been shown that chaotic transitions between attractors appear in the process of learning odors in the olfactory bulb of rabbits; this discovery was crucial for elucidating the role of chaos in neural information processing [6]. Chaotic transitory dynamics in the brain has been dealt with as chaotic itinerancy in relation to heteroclinic cycles and blowout bifurcations [7]. Transient dynamical models for odor representation in olfactory systems, referred to as winnerless competition networks, have also been studied recently [8]. Their transient patterns are robust and sensitive to stimuli and are based on heteroclinic sequences connecting multiple steady states. Transients, the duration of which increase exponentially with the number of neurons, have also been found in several neural network models. With respect to chaotic transients (supertransients), various groups have studied stable chaos in diluted random networks of integrate-and-fire neurons with excitatory [9] and inhibitory [10] coupling, the edge of chaos in discrete time recurrent networks of spiking neurons [11], self-sustained asynchronous irregular activity states in networks of spiking neurons with conductance-based synapses [12], and rotating waves in a ring of Bonhoeffer-van der Pol models [13]. For other kinds of exponential transients, transient states before reaching periodic orbits in asymmetric Hopfield networks [14], iteration processes in neuronal recurrence equations [15], and transient well-controlled sequences in continuous-time Hopfield networks [16] have been studied.

Recently, the authors have shown metastable dynamical transient rotating waves and oscillations in a ring of unidirectionally coupled sigmoidal neurons [17,18]. The propagation of their wave fronts is described with qualitatively the same kinematical equation as the above-mentioned bistable reaction-diffusion systems. It has been shown that the duration of transient rotating waves increases exponentially with the initial bump width, the duration of randomly generated rotating waves obeys a power-law distribution, and spatiotemporal

\*Corresponding author: horikawa@eng.kagawa-u.ac.jp

noise with intermediate strength can increase the duration of transient rotating waves. Studies on networks of sigmoidal neurons date back to the early 1970s [19]. Originally the sigmoidal function was introduced as the activity of a population of neurons. It was then employed as a simple model of a single neuron, which reflects its firing rate or frequency. Much work has since been carried out on the dynamics of the networks of sigmoidal neurons, e.g., associative memory [20]. Pattern formation in one- and two-dimensional arrays of sigmoidal neurons has been extensively studied; these arrays are referred to as cellular neural networks [21]. Long-lasting transient spatiotemporal patterns in two-dimensional cellular neural networks have also been demonstrated with computer simulation [22]. They consist of separated regions with slowly moving boundaries, which are similar to those in the bistable reaction-diffusion systems. However, they might not have exponentially long duration, as discussed in Appendix A in this paper, since a piecewise linear function is employed as an output function of a neuron for mathematical analysis. Further, various spatiotemporal patterns in rings of sigmoidal neurons with delays have been studied [23]. It has also been shown that rings of unidirectionally coupled sigmoidal neurons show long-lasting transients in the presence of delays [24]. However, their duration does not seem to be exponentially dependent on the number of neurons.

More interestingly, metastable dynamical transient rotating waves have been found in a ring of unidirectionally coupled Bonhoeffer-van der Pol neuron models, i.e., spiking neurons, in the form of propagating oscillations [25]. Neurons are connected with slow inhibitory synapses, the time constant of which is more than 10 times smaller than that of a recovery variable. In the asymptotically stable states of the system, neurons in firing states and resting states are located alternately in the ring. In transient states, there are two inconsistencies at which successive two neurons are in the same state, and their locations propagate in the direction of coupling. Then each neuron alternates between a firing state and resting state until it settles down in one of the states eventually. The propagation of the locations of the inconsistencies is described by the same kinematics as that in a ring of sigmoidal neurons, which derives the exponentially long duration of transient propagating oscillations.

To the best of the author's knowledge, metastable dynamical transients having a duration that increases exponentially with the number of neurons in a neural network model have been shown only in the form of rotating waves in rings of unidirectionally coupled neurons, as mentioned above [17,18,25]. A ring with unidirectional coupling is a special structure, and there are bidirectional and self-coupling between neurons as well as between populations of neurons in general. In the central nervous system, for instance, lateral inhibition in the visual pathway, projections between the entorhinal cortex and CA1 cells in the hippocampus, interactions between Purkinje cells and basket cells in the cerebellum cortex and interactions between populations of pyramidal cells are well known [26]. Bidirectional interactions have been found even between neurons and astrocytes [27]. Further, various models have been studied for central pattern generators, which generate periodic oscillations for rhythmic motion such as walking, flying, and swimming, e.g., [28] for early work.

Most of them consist of closed loops of neurons including bidirectional coupling.

In this paper, we consider transient dynamics and patterns in a ring of bidirectionally coupled sigmoidal neurons. It is expected that metastable dynamical transient patterns will emerge because of the symmetric bistability of the system being considered. Since the neuron model is simple, the dynamics of the system can be analyzed in the same manner as that of a ring of unidirectionally coupled sigmoidal neurons, and changes in transient patterns will be described kinematically. Obtained results will help to study effects of bidirectional coupling on metastable dynamical firing patterns in a ring of spiking neurons. Also, its analysis will provide new insight into transient dynamics in artificial neural networks. It is shown that a pair of stable spatially uniform steady solutions is generated from the origin as the gain of the sigmoidal output function of a neuron increases and the system becomes bistable. Pairs of unstable spatially nonuniform symmetric steady solutions are generated from the origin through pitchfork bifurcations successively as the gain increases further. The unstable spatially nonuniform solutions with zero-state neurons are then stabilized. Pairs of stable and unstable spatially nonuniform asymmetric steady solutions are also generated through saddle-node bifurcations. When the system is bistable, the instability of the spatially nonuniform symmetric solutions decreases exponentially with the number of neurons. That is, the largest eigenvalues of the Jacobian matrices evaluated at the solutions decrease exponentially with the number of neurons. This exponentially weak instability of the symmetric solutions is responsible for the emergence of metastable dynamical patterns. It is shown with computer simulation that the duration of spatially nonuniform patterns increases exponentially with the initial width of a smaller bump and the duration of randomly generated patterns obeys a power-law distribution. These simulation results are well explained using a kinematical equation for changes in bump width.

We also consider three effects on metastable dynamical transient patterns. The first is small spatial variations in coupling strength. It is shown with computer simulation that small random variations in coupling strength easily stabilize spatially nonuniform steady patterns. Changes in the bifurcations of spatially nonuniform solutions that cause their stabilization are then shown. The second effect is asymmetry in the direction of coupling. Unstable traveling-wave solutions instead of steady solutions are generated from the origin through Hopf bifurcations when coupling is asymmetric. They then change into steady solutions through pinning as the gain of the output function of a neuron increases. It is shown that the duration of transient waves rotating in a ring also increases exponentially with initial bump width and the growth rate depends on the asymmetry in coupling. The third effect is asymmetry in the output function of a neuron. It is shown that the largest eigenvalues of spatially nonuniform symmetric solutions increase as the asymmetry becomes large. The duration of spatially nonuniform patterns then increases only linearly with the initial width of a smaller bump.

Further, transient patterns in a two-dimensional array of symmetrically coupled neurons are considered. It is shown that spatially nonuniform solutions with one-dimensional

forms are dominant and a power-law distribution of randomly generated patterns is described by the kinematical equation in a one-dimensional ring of neurons. Although long-lasting transient patterns have been reported in two-dimensional cellular neural networks as mentioned above, metastable dynamical transient patterns with these properties have not been shown.

The rest of the paper is organized as follows. A model equation of a ring of bidirectionally coupled sigmoidal neurons and the bifurcations and properties of its solutions are explained in Sec. II. In Sec. III, a kinematical equation for a change in the width of bumps in spatially nonuniform patterns is described. Metastable dynamics of spatially nonuniform patterns are then demonstrated by computer simulation, and it is found that the solutions to the kinematical equation agree with the simulation results. In the following three sections, Secs. IV–VI, the effects of variations in coupling strength, asymmetry in the direction of coupling, and asymmetry in the output function on metastable dynamical transient patterns are examined. Transient patterns in a two-dimensional array of symmetrically coupled neurons are considered in Sec. VII. Application of the obtained results to networks of spiking neurons and other systems is discussed in Sec. VIII. Finally, a conclusion and consideration of future work are given in Sec. IX. The duration of transient patterns in a cellular neural network with a piecewise linear output function is also shown in Appendix A. Remarks on bifurcations and metastable dynamical patterns in open chains of neurons are provided in Appendix B.

## II. A RING OF BIDIRECTIONALLY COUPLED SIGMOIDAL NEURONS AND ITS BIFURCATION

### A. A model and the bifurcation of the origin

We consider the following model of a ring of bidirectionally coupled sigmoidal neurons:

$$\begin{aligned} dx_n/dt &= -x_n + c_{n,n-1}f(gx_{n-1}) + c_{n,n+1}f(gx_{n+1}) \\ f(x) &= \tanh(x) \quad (1 \leq n \leq N, x_{n\pm N} = x_n, c_{n\pm N, n' \pm N} = c_{n, n'}), \end{aligned} \quad (1)$$

where  $x_n$  is the state of the  $n$ th neuron,  $f$  is the output function of a neuron,  $g$  ( $\geq 0$ ) is an output gain, and  $c_{n, n'}$  is coupling strength from the  $n$ th neuron to the  $n'$ th neuron. A periodic boundary condition is imposed so a total of  $N$  neurons make a closed loop with bidirectional nearest-neighbor coupling. In this and the next sections, we consider the following symmetric bidirectional coupling:

$$c_{n, n-1} = c_{n, n+1} = 1/2 \quad (1 \leq n \leq N, c_{n\pm N, n' \pm N} = c_{n, n'}). \quad (2)$$

Equation (1) has two kinds of symmetry with Eq. (2). One is  $\mathbf{Z}_2$  symmetry: Equation (1) is invariant to changes in the signs of variables,  $x_n \rightarrow -x_n$  ( $1 \leq n \leq N$ ), since  $f(x)$  is an odd function [ $f(-x) = -f(x)$ ]. Hence, if  $x_n$  ( $1 \leq n \leq N$ ) is a solution to Eq. (1), then  $-x_n$  ( $1 \leq n \leq N$ ) is always a solution to Eq. (1). The other is the spatial symmetry of the dihedral group  $\mathbf{D}_n$  due to identical neurons and symmetric nearest-neighbor coupling [29]. Hence, the solutions are invariant to shifts and reflection in  $n$ : If  $x_n$  ( $1 \leq n \leq N$ ) is a solution to Eq. (1), then

$x_{n+n'}$  and  $x_{-n}$  ( $1 \leq n \leq N, x_{n\pm N} = x_n$ ) are also solutions to Eq. (1).

The stability of a steady solution [ $x_n(t) = x_n$  ( $1 \leq n \leq N$ )] of Eq. (1) is evaluated with the following Jacobian matrix  $A$ .

$$A = \begin{bmatrix} -1 & c_{1,2}f'_2 & & & c_{1,N}f'_N \\ c_{2,1}f'_1 & -1 & c_{2,3}f'_3 & & \\ & & & & \\ c_{N,1}f'_1 & & & c_{N,N-1}f'_{N-1} & -1 \end{bmatrix} \times (f'_n = f'(gx_n) = g \operatorname{sech}^2(gx_n)). \quad (3)$$

The origin [ $x_n = 0$  ( $1 \leq n \leq N$ )] is always a steady solution and the eigenvalues  $\lambda_k$  of  $A$  with Eq. (2) evaluated at the origin are given by

$$\lambda_k = -1 + g \cos(2k\pi/N) \quad (0 \leq k < N). \quad (4)$$

The origin is then stable when  $0 \leq g < 1$  and is destabilized at  $g = g_0 = 1$  ( $\lambda_0 = -1 + g_0 = 0$ ) through a pitchfork bifurcation due to the  $\mathbf{Z}_2$  symmetry of Eq. (1). A pair of stable spatially uniform states,  $x_n = \pm x_s$  ( $1 \leq n \leq N$ ) with  $x_s = \tanh(gx_s)$ , is then generated and they are always stable when  $g > 1$ , since  $f'_n \rightarrow 0$  as  $g \rightarrow \infty$ . As  $g$  increases further, a pair of the eigenvalues ( $\lambda_1$  and  $\lambda_{N-1}$ ) becomes zero at  $g = g_1 = 1/\cos(2\pi/N)$  when  $N \geq 5$ . Two pairs of unstable spatially nonuniform solutions with the wave number  $k = 1$  are then generated at the same time through a degenerate pitchfork bifurcation. A further increase in  $g$  causes successive pitchfork bifurcations at the origin, and pairs of spatially nonuniform solutions with the wave number  $k$  are generated when pairs of the eigenvalues ( $\lambda_k$  and  $\lambda_{N-k}$ ,  $2 \leq k < N/4$ ) become zero. All these spatially nonuniform solutions are unstable at their generation and their unstable dimensions are  $2k - 1$  and  $2k$ .

### B. Bifurcations in rings with $N = 6, 7$ , and $8$

The bifurcations of solutions and the generation of stable spatially nonuniform solutions in rings of small numbers of neurons are shown. The properties of bifurcations in rings of large numbers of neurons can be understood qualitatively from these bifurcations and solutions. Bifurcations of Eq. (1) were calculated with the software package AUTO [30] as well as computer simulation of Eq. (1) with the Runge-Kutta method and a time step of 0.01.

Figure 1(a) shows a bifurcation diagram of Eq. (1) with  $N = 6$ , in which the state ( $x_n$ ) of one neuron against the output gain  $g$  is plotted. The branches of stable (unstable) solutions are plotted with thick (thin) lines. The numbers (0, 1, 2) located along branches are the unstable dimensions of solutions. The origin is destabilized at  $g = g_0 = 1$  and a pair of stable spatially uniform steady solutions [ $\pm x_s$  ( $1 \leq n \leq N$ )] is generated. Two branches corresponding to  $\lambda_1$  and  $\lambda_{N-1}$  are then generated from the origin at  $g = g_1 = 2.0$ . One is referred to as type 2, in which  $x_3 = x_6 = 0$ ,  $x_1 = x_2 > 0$ , and  $x_4 = x_5 (= -x_1) < 0$  (plotted with a solid line), which is one-dimensionally unstable at generation. The other is referred to as type 0, in which  $x_n > 0$  ( $1 \leq n \leq 3$ ) and  $x_n < 0$  ( $4 \leq n \leq 6$ ) (plotted with a dashed line), which is two-dimensionally unstable. Note that type  $n$  indicates that the number of neurons

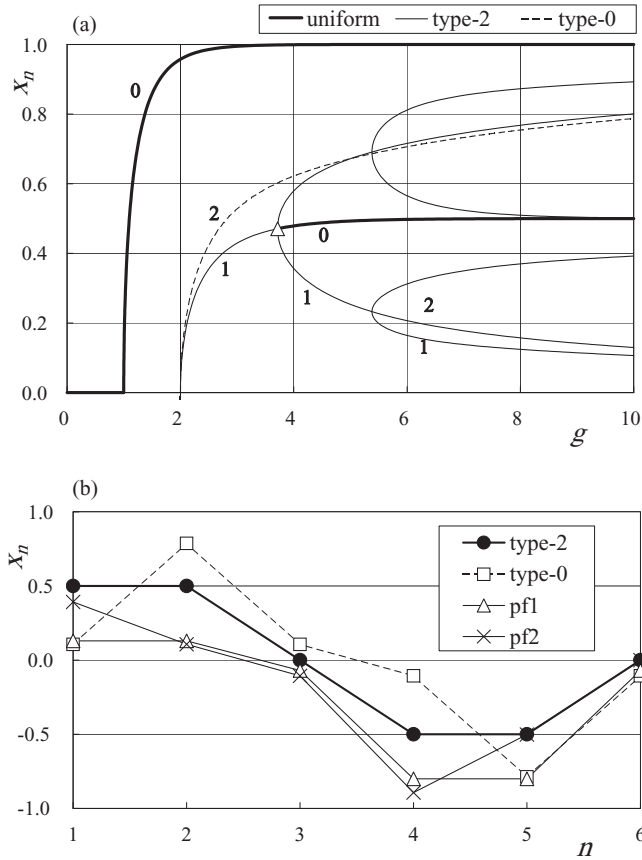


FIG. 1. (a) Bifurcation diagram of Eqs. (1) and (2) with  $N = 6$ . The state ( $x_n$ ) of one neuron vs the output gain  $g$ . Stable solutions (thick lines), unstable solutions (thin lines), and the pitchfork bifurcation point  $g_{PF}$  (triangle). Numbers (0, 1, 2) are unstable dimensions. (b) Examples of spatial patterns of solutions at  $g = 10$ . Type 2 (solid circles with a thick solid line), type 0 (open squares with a dashed line), and spatially asymmetric solutions pf1, pf2 (triangles and crosses with solid lines).

with zero states in the solution is  $n$ . Figure 1(b) shows examples of spatial patterns of these solutions at  $g = 10$ , in which the type 2 and type 0 solutions are plotted with solid circles connected with a thick solid line and open squares connected with a dashed line, respectively. They are located in the invariant subspace,  $x_{n+N/2} = -x_n$  ( $1 \leq n \leq N/2$ ), because of the  $\mathbf{Z}_2$  and spatial  $\mathbf{D}_n$  symmetry of Eqs. (1) and (2). The size of the two (positive and negative) bumps in these solutions is the same, and thus they are spatially symmetric. The type 2 solution is then stabilized at  $g = g_{PF} = 3.72$  through a subcritical pitchfork bifurcation (plotted with an open triangle) and a pair of spatially asymmetric solutions are generated. A further increase in  $g$  causes a pitchfork bifurcation of a pair of asymmetric solutions at  $g = 5.38$ , but it is supercritical and stable solutions are not generated. Examples of spatial patterns of generated unstable spatially asymmetric solutions are also plotted with triangles and crosses connected with solid lines in Fig. 1(b) (pf1, pf2). The type 0 solution is neither bifurcated nor stabilized as  $g$  increases.

When the number  $N$  of neurons is odd, spatially nonuniform solutions with different forms are generated from the origin. Figure 2 shows a bifurcation diagram of Eq. (1) with  $N = 7$

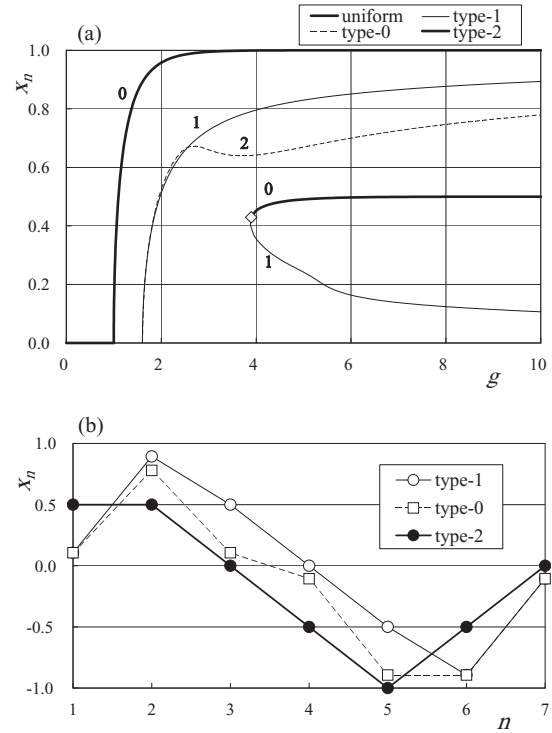


FIG. 2. (a) Bifurcation diagram of Eqs. (1) and (2) with  $N = 7$ . The state ( $x_n$ ) of one neuron vs the output gain  $g$ . Stable solutions (thick lines), unstable solutions (thin lines), and the saddle-node bifurcation point  $g_{SN}$  (diamond). Numbers (0, 1, 2) are unstable dimensions. (b) Examples of spatial patterns of solutions at  $g = 10$ . Type 1 (open circles with a solid line), type 0 (open squares with a dashed line), and type 2 (solid circles with a thick solid line).

[Fig. 2(a)] and examples of spatial patterns of solutions at  $g = 10$  [Fig. 2(b)]. Two pairs of spatially nonuniform solutions are generated from the origin at  $g = g_1 = 1.60$  through a degenerate pitchfork bifurcation. One is spatially symmetric and of type 1 with one zero-state neuron and two symmetric positive and negative bumps consisting of  $(N - 1)/2$  neurons and is plotted with open circles connected with a solid line in [Fig. 2(b)]. The other is asymmetric and of type 0 with two (positive and negative) bumps consisting of  $(N - 1)/2$  and  $(N + 1)/2$  neurons and is plotted with open squares connected with a dashed line in Fig. 2(b). Both solutions are not bifurcated and remain unstable as  $g$  increases. Instead, a pair of stable and unstable solutions is generated through a saddle-node bifurcation at  $g = g_{SN} = 3.88$  (an open diamond). The stable solution is of type 2 and has two (positive and negative) bumps consisting of  $(N - 3)/2$  and  $(N - 1)/2$  neurons and two zero-state neurons at their boundaries, while the unstable solution is of type 1 and has two bumps consisting of  $(N - 3)/2$  and  $(N + 1)/2$  neurons and one zero-state neuron at one boundary. The stable type 2 solution is plotted with closed circles connected with a thick solid line in Fig. 2(b).

When  $N = 8$ , two pairs of unstable spatially symmetric solutions (type 0, 2) are generated from the origin at  $g = 1.41$  and the type 2 solution is stabilized through a pitchfork bifurcation at  $g = 2.46$  in the same manner as  $N = 6$ . In addition, a stable spatially asymmetric solution is generated through a saddle-node bifurcation at  $g = 3.88$ . This solution

has two zero-state neurons and two (positive and negative) bumps consisting of  $N/2 - 2$  and  $N/2$  neurons, i.e., it is a type 2 solution. Two pairs of stable spatially nonuniform solutions thus coexist with a pair of stable spatially uniform solutions ( $\pm x_s$ ).

### C. Stability of spatially nonuniform solutions

Pairs of the eigenvalues  $[\lambda_k$  and  $\lambda_{N-k}$  ( $2 \leq k < N/4$ )] of the Jacobian matrix  $A$  evaluated at the origin become positive as  $g$  increases when  $N \geq 9$ . Pairs of unstable spatially periodic solutions with the wave number  $k \geq 2$  are generated, in which there are  $k$  pairs of positive and negative bumps. When  $N = 2(3+m)k$  ( $m$ : nonnegative integer), i.e.,  $N/k$  is even and six or more, the generated solutions of type- $2k$  are also stabilized through pitchfork or transcritical bifurcations  $k$  times ( $k-1$  of them are degenerate) as  $g$  increases. They consist of  $k$  pairs of positive and negative bumps with  $2+m$  neurons and  $2k$  zero-state neurons at boundaries, and the states of the neurons are  $(-1)^k x_{n+k'(3+m)}$  ( $1 \leq n \leq 3+m$ ,  $0 \leq k' \leq 2k-1$ ) with  $x_{k'(3+m)} = 0$  ( $1 \leq k' \leq 2k$ ). The value of  $g$  at the  $k$ th time bifurcation (at the stabilization) depends only on  $m$ , not on  $k$ , i.e., it depends on the width ( $2+m$ ) of bumps. In addition, spatially asymmetric solutions, in which a smaller bump consists of at least two neurons of nonzero states, are generated through saddle-node bifurcations. Further, solutions with more than one pair of positive and negative bumps with various widths are generated through saddle-node bifurcations, so many stable solutions coexist when  $N$  and  $g$  are large. Stabilized spatially nonuniform solutions have one or more pairs of positive and negative one-peak symmetric bumps consisting of two or more nonzero state neurons, which are separated by zero-state neurons, i.e., they are of type  $2k$  ( $k \geq 1$ ). In the limit of  $g \rightarrow \infty$ , spatial patterns of the states  $x_n$  of neurons in stable spatially nonuniform solutions consist of even numbers of bumps of arbitrary (including zero) length of 1 or  $-1$  and  $\{\pm 1/2, 0, \mp 1/2\}$  at the boundaries between bumps. That is,  $(-1/2, -1 \times m, -1/2, 0, 1/2, 1 \times m, 1/2, 0) \times k$ , where  $\times m$  and  $\times k$  mean  $m$  and  $k$  successions of the left elements, respectively.

The value of the output gain  $g_{PF}$  at which the type 2 solution is stabilized decreases to unity as the number  $N$  of neurons increases as well as the value  $g_1$  [ $=1/\cos(2\pi/N)$ ] at which the unstable solutions (types 0, 1, 2) with the wave number  $k=1$  are generated through the Hopf bifurcation from the origin. The value  $g_{SN}$  at which the stable spatially asymmetric type 2 solution with bumps of  $(N-3)/2$  and  $(N-1)/2$  neurons is generated through a saddle-node bifurcation for odd  $N$  also decreases to unity as  $N$  increases. Figure 3 shows a semilog plot of  $g_1 - 1$ ,  $g_{PF} - 1$  (for even  $N$ ) and  $g_{SN} - 1$  (for odd  $N$ ) against the number  $N$  of neurons with solid circles, open circles, and open squares, respectively. The values of  $g_{SN} - 1$  for odd  $N$  (open squares) are only slightly larger than  $g_{PF} - 1$  for even  $N$  (open circles), and both decrease with  $N$ . When  $g_1 < g < g_{PF}$  for even  $N$  and when  $g_1 < g < g_{SN}$  for odd  $N$ , the unstable spatially nonuniform solutions coexist with a pair of stable spatially uniform solutions.

It can also be shown that the values  $g_{PF}$  of the symmetric type 2 solution and the values  $g_{SN}$  of the asymmetric type 2 solutions with the same width of a smaller bump are almost

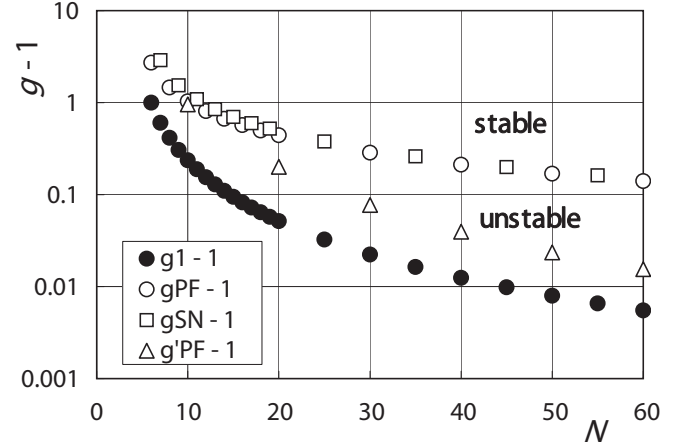


FIG. 3. Semilog plot of  $g_1 - 1$  (solid circles),  $g_{PF} - 1$  for even  $N$  (open circles),  $g_{SN} - 1$  for odd  $N$  (open squares), and  $g'_{PF} - 1$  (open triangles) vs the number  $N$  of neurons.

the same irrespective of  $N$ . That is, the stability of the type 2 solutions is almost the same irrespective of the width of a larger bump. When a smaller bump consists of two positive neurons with zero-state neurons on both sides, then, for example,  $g_{PF} = 3.72$  (the symmetric type 2 solution) when  $N = 6$  and  $g_{SN} = 3.88$  (the asymmetric type 2 solutions) when  $N = 7, 8, 9, \dots$ . The stability of the type 2 solutions thus depends mainly on the width of a smaller bump, and the values of  $g_{PF}$  and  $g_{SN}$  decrease with the number of the neurons in a smaller bump. For a fixed  $g$ , if the symmetric type 2 solution with the bump width  $N/2$  is generated (stabilized) in a ring of  $N$  neurons, the asymmetric type 2 solutions with the same width of a smaller bump are also generated (stabilized) in a ring of more than  $N$  neurons.

Figure 4 then shows a semilog plot of the largest eigenvalue  $\mu$  of the Jacobian matrix  $A$  [Eq. (3)] evaluated at the unstable type 2 and type 1 solutions against the number  $N$  of neurons at  $g = 1.1$  (circles),  $1.2$  (squares),  $1.5$  (triangles), and  $2.0$  (diamonds). The values for type 2 ( $N$ : even) and type 1 ( $N$ : odd) are plotted with solid and open symbols, respectively. The largest eigenvalue decreases exponentially as the number  $N$  of neurons increases until the type 2 solution for even  $N$  is stabilized. The eigenvalue of the type 1 solution (open

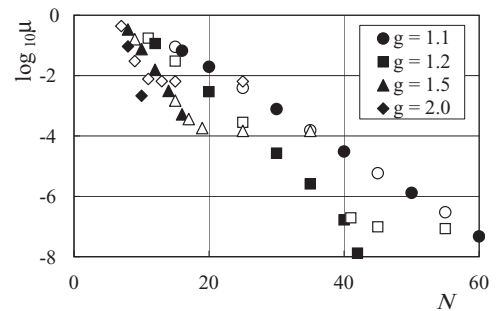


FIG. 4. Semilog plot of the largest eigenvalue  $\mu$  of the Jacobian matrix  $A$  evaluated at the unstable type 2 ( $N$ : odd) and type 1 ( $N$ : even) solutions to Eqs. (1) and (2) vs the number  $N$  of neurons at  $g = 1.1$  (circles),  $1.2$  (squares),  $1.5$  (triangles), and  $2.0$  (diamonds). Type 2 (solid symbols) and type 1 (open symbols).

symbols) for odd  $N$  remains at about the same value after the stabilization of the type 2 solution, even though  $N$  increases further, e.g.,  $g = 1.2$  at  $N = 45, 55$  (an open square). (The largest eigenvalue of the type 0 solution is the same as that of the type 2 (type 1) solution for even (odd)  $N$  when the type 2 solution is unstable.) These weakly unstable spatially nonuniform solutions, which have exponentially small largest eigenvalues, cause metastable dynamical transient patterns, the duration of which increases exponentially with the number of neurons.

### III. METASTABLE DYNAMICAL TRANSIENT PATTERNS

In this section, we consider transient states of Eq. (1) with Eq. (2) for small  $g$  ( $>1$ ), in which Eq. (1) is bistable and spatially nonuniform solutions are unstable. It is shown that transient spatially nonuniform patterns show metastable dynamics. Their duration increases exponentially with the number of neurons and the duration of randomly generated patterns is distributed in a power-law form.

#### A. Kinematical equations for a change in bump width

In analogy to kink-antikink interactions in a bistable reaction-diffusion equation [1] and pulse propagation in a ring of unidirectionally coupled sigmoidal neurons [17], we derive an equation for a change in bump size in transient patterns. We consider a range of the output gain:  $g_1 < g < g_{PF}$  for even  $N$  and  $g_1 < g < g_{SN}$  for odd  $N$ , in which Eq. (1) has a pair of stable spatially uniform solutions and pairs of unstable spatially nonuniform solutions while it has no stable spatially nonuniform solutions. Let a pair of positive and negative bumps exist in a ring of  $N$  neurons and let the locations of boundaries between them be  $l_1$  and  $l_2$  ( $0 < l_1 < l_2 \leq N$ ). The widths of bumps is then  $l = l_2 - l_1 \pmod{N}$  and  $N - l$ , which correspond to the numbers of neurons in bumps. We consider a continuous limit in space and let  $l_1, l_2$ , and  $l$  be real numbers. According to Ref. [1], the motion of the boundaries can be described by the following kinematical equation:

$$dl_n/dt = (-1)^n \beta/2 \{ \exp[-\alpha(N-l)] - \exp(-\alpha l) \} \\ (n \in \{1, 2\}, \alpha, \beta > 0, 0 < l_1 < l_2 \leq N, 0 < l < N). \quad (5)$$

Although there is no analytical derivation of Eq. (5) for this spatially discrete system, a qualitatively identical equation has been derived in the case of unidirectional coupling [17]. There is interaction between the boundaries, and its strength decreases exponentially with the distance between the boundaries, which arises from the difference in the bump width. This interaction makes the boundaries move right (left) when the width of a right (left) bump is smaller than the other. As a result, the width of a smaller bump decreases and the smaller bump disappears eventually so the state reaches one of the stable spatially uniform solutions.

A change in the bump width is then described by

$$dl/dt = \beta \{ \exp[-\alpha(N-l)] - \exp(-\alpha l) \} \quad (0 < l < N). \quad (6)$$

Equation (6) has an unstable steady solution  $l(t) = N/2$ , which corresponds to the spatially nonuniform symmetric solution to

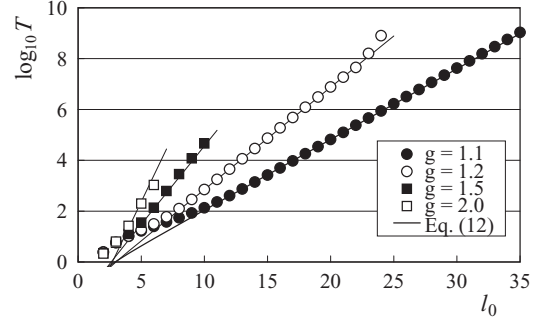


FIG. 5. Semilog plot of the duration  $T$  of transient patterns in Eqs. (1) and (2) vs the initial width  $l_0$  of a smaller bump. Results of computer simulation with  $g = 1.1$  (solid circles),  $1.2$  (open circles),  $1.5$  (solid squares),  $2.0$  (open squares), and Eq. (12) (solid lines).

Eq. (1). In this sense, Eqs. (5) and (6) can be applied when the spatially nonuniform solutions with the bump width  $l$  exist in Eq. (1) and they are unstable, hence,  $g_1 < g < g_{PF}$  for even  $N$  and  $g_1 < g < g_{SN}$  for odd  $N$ , as shown in Fig. 3. An equation for the perturbation  $l' = l - N/2$  in Eq. (6) is

$$dl'/dt = \beta \exp(-\alpha N/2) [ \exp(\alpha l') - \exp(-\alpha l') ] \\ \approx 2\alpha\beta \exp(-\alpha N/2) l' \quad (l' \ll 1). \quad (7)$$

The coefficient of  $l'$  in Eq. (7) can be approximated by the largest eigenvalue  $\mu$  of the Jacobian matrix  $A$  evaluated at the spatially nonuniform solution to Eq. (1), i.e.,  $\mu = 2\alpha\beta \exp(-\alpha N/2)$ . The values of  $\alpha$  and  $\beta$  in Eqs. (5) and (6) are thus estimated by fitting the graph of  $\mu$  vs  $N$  in Fig. 4 with this relation.

#### B. Exponential increases in the duration of transient patterns

The solution  $l(t)$  to the kinematical equation (6) under the initial condition  $l(0) = l_0$  is obtained as [17]

$$\exp(-\alpha |l(t) - N/2|) \\ = \tanh\{-\exp(-\alpha N/2)\alpha\beta t \\ + \operatorname{arctanh}[\exp(-\alpha |l_0 - N/2|)]\} \quad (l(0) = l_0). \quad (8)$$

The duration  $T$  of transient patterns is obtained by letting  $l(T) = 0$  under  $l_0 < N/2$  or  $l(T) = N$  under  $l_0 > N/2$ , i.e.,  $|l(T) - N/2| = N/2$  in Eq. (8),

$$T = \exp(\alpha N/2)/(\alpha\beta) \{ \operatorname{arctanh}[\exp(-\alpha |l_0 - N/2|)] \\ - \operatorname{arctanh}[\exp(-\alpha N/2)] \}. \quad (9)$$

Simple forms of Eqs. (6), (8), and (9) are given by letting  $N$  be infinity ( $N \rightarrow \infty$ ) in Eq. (6) as

$$dl/dt = -\beta \exp(-\alpha l), \quad (10)$$

$$l(t) = 1/\alpha \log[\exp(\alpha l_0) - \alpha\beta t] \quad (l(0) = l_0 < N/2), \quad (11)$$

$$T = [\exp(\alpha l_0) - 1]/(\alpha\beta) \quad (l(T) = 0), \quad (12)$$

where  $l$  is the width of a smaller bump. The duration  $T$  of transient patterns thus increases exponentially with the initial width  $l_0$  of a smaller bump, i.e., the number of neurons in a smaller bump.

Figure 5 shows a semilog plot of the duration  $T$  of transient patterns against the initial width  $l_0$  of a smaller bump, which

was obtained by computer simulation of Eq. (1) with  $g = 1.1$  (solid circles), 1.2 (open circles), 1.5 (solid squares), and 2.0 (open squares). Equation (1) was numerically calculated with the Runge-Kutta method and a time step of 0.01. The numbers of neurons were  $N = 80$  ( $g = 1.1$ ), 60 ( $g = 1.2$ ), and 40 ( $g = 1.5, 2.0$ ). The initial condition was given by

$$x_n = -1 (1 \leq n \leq l_0), x_n = 1 (l_0 + 1 \leq n \leq N). \quad (13)$$

The value of the duration  $T$  was obtained as a time at which the signs of the states of all neurons became the same, after which the state quickly converged to the spatially uniform solution. Equation (12) is also plotted with solid lines in Fig. 5. The values of  $\alpha$  and  $\beta$  are estimated with the relation  $\mu = 2\alpha\beta\exp(-\alpha N/2)$  in Eq. (7) and the graph of the eigenvalue  $\mu$  in Fig. 4 as mentioned above. The exponential growth rates are  $\alpha = 0.64, 0.93, 1.42,$  and  $2.38$  for  $g = 1.1, 1.2, 1.5,$  and  $2.0$ , respectively.

The duration  $T$  of spatially asymmetric patterns increases exponentially with the initial bump width  $l_0$  in some ranges. The range of  $l_0$  in which  $T$  increases exponentially depends on the applicability of Eqs. (5) and (6) to Eq. (1), i.e.,  $g_1 < g < g_{PF}, g_{SN}$ . The exponential increase in  $T$  thus appears in the region in which the unstable solutions exist in Fig. 3, which lies between the lines of the solid circles ( $g_1$ ) and open ( $g_{PF}, g_{SN}$ ) circles and squares. For fixed  $l_0$ , the solution with the bump width  $l_0 (=N/2)$  must exist (a lower bound) and be unstable (an upper bound). For a fixed output gain  $g$ , the lower (upper) bound of  $l_0$  is given by a half ( $=N/2$ ) of the number  $N$  of neurons at which a line of solid circles (open circles and squares) crosses a horizontal line at  $g$  in Fig. 3. (Actually, the upper bound of  $l_0$  in Fig. 5 is larger than the corresponding  $N/2$  by one or two since the initial condition [Eq. (13)] is not the same as the type 2 solution to Eq. (1).) The range of  $l_0$  for the exponential increase in  $T$  is large when the output gain is small:  $7 < l_0 < \text{over } 30$  for  $g = 1.1$ ;  $5 < l_0 < 22$  for  $g = 1.2$ . The duration of transient patterns then reaches  $T \sim 10^8$ . However, the range for the exponential increase becomes narrow and the maximum duration becomes small ( $10^3 < T < 10^5$ ) as the output gain increases ( $g = 1.5, 2.0$ ). The lines of Eq. (12) derived from the kinematical equation (10) agree with the simulation results in the range of  $l_0$  for the exponential increase in  $T$ .

On the other hand, the exponential growth rate  $\alpha$  increases with the output gain  $g$ . Figure 6 shows the growth rate  $\alpha$  of the duration  $T$  against  $g$ . Plotted are estimates with the relation  $\mu = 2\alpha\beta\exp(-\alpha N/2)$  in Eq. (7) and the graph of the eigenvalue  $\mu$  vs  $N$  (solid circles) and approximation by  $\alpha = 2.5(g - 1)^{0.6}$  (a solid line). The growth rate increases in proportion to the power of  $g - 1$ . The duration of spatially asymmetric patterns can more rapidly increase with the initial bump width as  $g$  becomes larger, unless they are stabilized.

The existence of an unstable spatially nonuniform symmetric solution is responsible for the occurrence of these metastable dynamical patterns. The exponential increase in the duration of transient patterns is attributed to the exponential decrease in the largest eigenvalue of the Jacobian matrix  $A$  evaluated at the unstable symmetric solution. In a cellular neural network (CNN) with a piecewise linear output function, spatially nonuniform solutions are always stable if they exist and there are no unstable solutions [22]. Then the duration

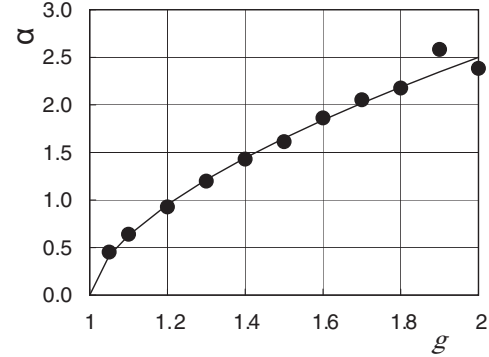


FIG. 6. Growth rate  $\alpha$  of the duration  $T$  of transient patterns vs  $g$ . Estimates with the relation  $\mu = 2\alpha\beta\exp(-\alpha N/2)$  in Eq. (7) and the graph of the eigenvalue  $\mu$  vs  $N$  (solid circles) and approximation by  $\alpha = 2.5(g - 1)^{0.6}$  (a solid line).

of transient patterns does not increase exponentially with the number of neurons but only polynomially with that number. The results of computer simulation with CNN are shown in Appendix A.

Although arrays with a ring structure (under a periodic boundary condition) are considered here, metastable dynamical patterns appear under other boundary conditions when coupling is symmetric [Eq. (2)]. Bifurcations and transient patterns in open chains of neurons under Dirichlet and Neumann boundary conditions are shown in Appendix B.

### C. Power-law distributions of the duration of randomly generated patterns

Next, we consider the duration of transient patterns generated under a random initial condition. Figure 7 shows an example of snapshots of spatial patterns of the states of neurons in transient states. It was obtained with computer simulation of Eq. (1) with  $g = 1.2$  and  $N = 35$  under a random Gaussian initial condition with the mean zero and the variance  $0.1^2$ :  $x_n(0) \sim N(0, 0.1^2)$  ( $1 \leq n \leq N$ ). A spatial pattern with positive and negative bumps is quickly generated ( $t = 30$ ) from an initial random pattern ( $t = 0$ ). Its bump width changes very slowly ( $t: 30 \sim 20\,000$ ) and it approaches the spatially uniform steady solution rather suddenly ( $t: 23\,000 \sim 24\,000$ ). The width of such quickly generated bumps is considered to be distributed uniformly in  $(0, N)$ . The initial width  $l_0$  of a smaller bump in the kinematical equation is then distributed uniformly in  $(0, N/2)$ . The probability density function  $h(T)$  of the duration  $T$

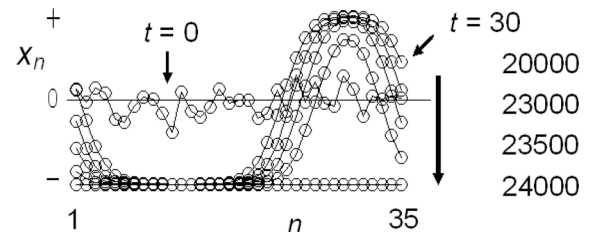


FIG. 7. Example of snapshots of spatial patterns of the states of neurons in transient states in Eqs. (1) and (2) with  $g = 1.2$  and  $N = 35$  under a random Gaussian initial condition:  $x_n(0) \sim N(0, 0.1^2)$  ( $1 \leq n \leq N$ ).

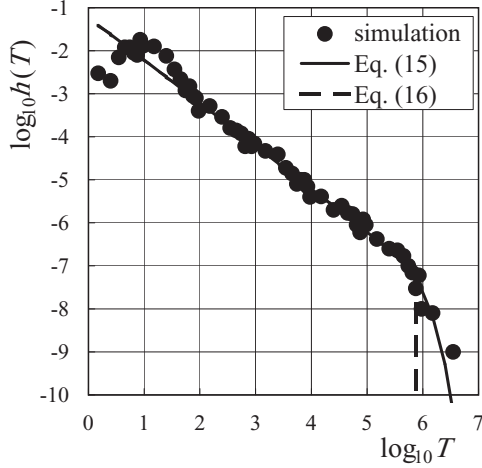


FIG. 8. Log-log plot of a normalized histogram  $h(T)$  of the duration  $T$  obtained with 1000 runs of computer simulation of Eqs. (1) and (2) with  $g = 1.2$  and  $N = 35$  under a random Gaussian initial condition:  $x_n(0) \sim N(0, 0.1^2)$  ( $1 \leq n \leq N$ ) (solid circles). Equations (15) (a solid line) and (16) (a dashed line) with  $\alpha = 0.93$  and  $\beta = 16.1$ .

of randomly generated patterns is derived with Eq. (9) as

$$\int_0^{l_0} U(0, N/2) dl'_0 = \int_0^T h(T') dT', \quad (14)$$

$$h(T) = \frac{1}{|dT(l_0; N)/dl_0|} \frac{2}{N} = \left| \frac{dl_0(T; N)}{dT} \right| \frac{2}{N}$$

$$= 4\beta \exp(-\alpha N/2) \operatorname{cosech}\{2[\exp(-\alpha N/2)\alpha\beta T + \operatorname{arctanh}(\exp(-\alpha N/2))]\} / N. \quad (15)$$

A simpler form is also obtained with Eq. (12) as

$$h(T) = \frac{\beta}{\alpha\beta T + 1} \frac{2}{N} \quad (0 < T < T_c = \exp(\alpha N/2)/(\alpha\beta)). \quad (16)$$

The duration of transient patterns is thus distributed in a power-law form ( $h(T) \sim 1/T$ ) up to a cut-off  $T_c$ .

Figure 8 shows a log-log plot of a normalized histogram of the duration  $T$  obtained with 1000 runs of the computer simulation of Eq. (1) with  $g = 1.2$  and  $N = 35$  under a random Gaussian initial condition:  $x_n(0) \sim N(0, 0.1^2)$  ( $1 \leq n \leq N$ ) (solid circles). Equations (15) and (16) with  $\alpha = 0.93$  and  $\beta = 16.1$  are also plotted with solid and dashed lines, respectively, and they agree with each other up to the cut-off:  $T_c = 7.8 \times 10^5$ . Finally, it should be noted that the mean and variance of the duration of randomly generated patterns also increase exponentially with the number of neurons (data not shown) [17].

#### IV. EFFECTS OF VARIATIONS IN COUPLING

In this section, we consider the effects of random variations in the strength of coupling on transient patterns in Eq. (1). It has been shown that propagating fronts are localized due to random spatial variations in reaction-diffusion systems, i.e., pinning occurs [31]. It has also been shown that random biases in the output functions of neurons degrade an exponential increase in the duration of transient rotating waves in a ring

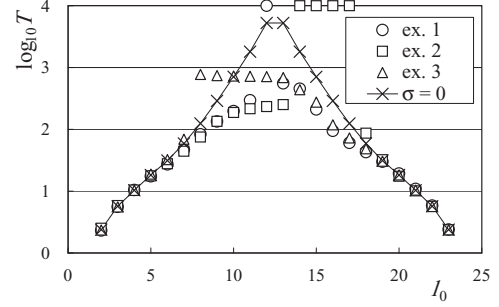


FIG. 9. Examples of the duration  $T$  of spatially nonuniform patterns in Eqs. (1) and (17) vs the initial width  $l_0$  of a smaller bump. Results of computer simulation with  $N = 25$ ,  $g = 1.2$ , and  $\sigma = 0.01$  under Eq. (13) [ex. 1 - 3 (open symbols)] and when  $\sigma = 0.0$  (crosses connected with a solid line). Plotted at  $T = 10^4$  are stabilized patterns.

of unidirectionally coupled sigmoidal neurons [18]. In the following it is shown that random variations in the coupling strength tend to stabilize spatially nonuniform patterns or to degrade the exponential increase in their duration in the same manner as these systems.

Instead of the symmetric bidirectional coupling [Eq. (2)], random variations are added to the strength of coupling between adjacent neurons as follows:

$$c_{n,n\pm 1} = 1/2 + \sigma w_{n,n\pm 1} \quad (1 \leq n \leq N, c_{n\pm N, n'\pm N} = c_{n,n'},$$

$$\sigma \geq 0)$$

$$E\{w_{n,n'}\} = 0, E\{w_{n_1, n'_1} w_{n_2, n'_2}\} = \delta_{n_1, n_2} \delta_{n'_1, n'_2}, \quad (17)$$

where  $w_{n,n'}$  is Gaussian white noise ( $\sim N(0, 1^2)$ ) and  $\sigma^2$  is the variance of random variations in coupling strength. The origin is still a steady solution to Eq. (1) with Eq. (17). The largest eigenvalue  $\lambda_0$  of the Jacobian matrix  $A$  of Eq. (1) evaluated at the origin is real and becomes positive at about  $g = 1.0$ , when  $\sigma$  is not much larger than  $1/2$ . A pair of stable nonzero (positive and negative) solutions is then generated through a pitchfork bifurcation due to the  $Z_2$  symmetry of Eq. (1), which is not spatially uniform but has random variations in the states  $x_n$  of neurons. The other degenerate eigenvalues become separated real eigenvalues or a pair of complex conjugate eigenvalues. A limit cycle is then generated through the Hopf bifurcation in the latter. Since bifurcations depend on individual patterns of variations in coupling strength, it is here shown that very small variations can stabilize spatially nonuniform solutions that would otherwise be unstable.

Figure 9 shows examples of the duration  $T$  of spatially nonuniform patterns against the initial width  $l_0$  of a smaller bump, which were obtained by computer simulation of Eqs. (1) and (17) with  $N = 25$ ,  $g = 1.2$ , and  $\sigma = 0.01$  under the initial condition Eq. (13). The duration in the absence of variations ( $\sigma = 0.0$ ) is plotted with crosses connected with a solid line. Plotted at  $T = 10^4$  are the cases when the states did not converge to one of stable positive and negative solutions at that time, which were thus considered to be stabilized (ex. 1, 2). Spatially nonuniform patterns are often stabilized in the presence of small variations ( $\sigma = 0.01$ ) in coupling strength. This occurs in the range of  $l_0$  for the exponential increase in  $T$  at about  $l_0 = T/2$ , in which spatially nonuniform solutions

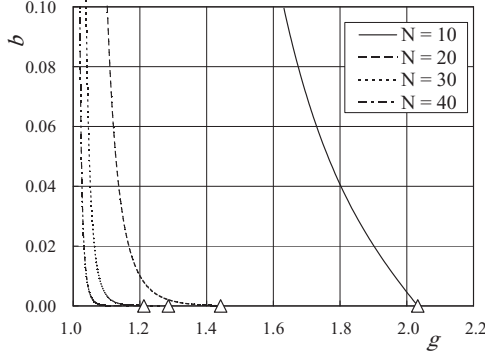


FIG. 10. Bifurcation diagram of Eqs. (1) and (18) in the  $g$ - $b$  plane. Loci of the pitchfork bifurcation points ( $g'_{\text{PF}}$ ,  $b'_{\text{PF}}$ ) of the symmetric type 2 solutions for  $N = 10$  (a solid line), 20 (a dashed line), 30 (a dotted line), and 40 (a dash-dotted line), and the pitchfork bifurcation points ( $g_{\text{PF}}$ , 0.0) (triangles).

exist in the absence of variations. Further, an increase in  $T$  tends to reach the ceiling if not stabilized (ex. 3). This degradation of the exponential increase in the duration of transient patterns is dealt with in Sec. VI. Random variations in coupling strength thus severely affect metastable dynamical transient patterns.

A simple example of changes in the bifurcations of Eq. (1) causing the stabilization of spatially nonuniform patterns is shown here. Consider the following bias in coupling strength at two points when the number  $N$  of neurons is even.

$$c_{N,1} = c_{N/2,N/2+1} = 1/2 - b, c_{n,n\pm 1} = 1/2 \text{ (otherwise)}. \quad (18)$$

As a bias  $b$  increases from zero to  $1/2$ , the coupling strength from the first neuron to the  $N$ th neuron and that from the  $N/2 + 1$ st neuron to the  $N/2$ nd neuron are reduced to zero. The eigenvalues of  $\lambda_k$  of the Jacobian matrix  $A$  evaluated at the origin remain real but become simple. When  $b = 1/2$ , they are obtained with  $N/2 \pm 1$  neurons under the Dirichlet boundary condition ( $x_0 = x_{N/2\pm 1} = 0$ ) as

$$\lambda_k = -1 + g \cos[k_{\pm} \pi / (N/2 \pm 1 + 1)] \quad (1 \leq k_{\pm} \leq N/2 \pm 1). \quad (19)$$

A pair of solutions generated from the origin through a pitchfork bifurcation at the largest eigenvalue  $\lambda_{1+} = 0$  has the states of neurons with the same sign and that generated at the second largest eigenvalue  $\lambda_{1-} = 0$  has the symmetric form of type 2. Then the first pitchfork bifurcation of the symmetric type 2 solution and its stabilization are still retained.

Figure 10 shows a bifurcation diagram in the  $g$ - $b$  plane, in which the loci of the pitchfork bifurcation points ( $g'_{\text{PF}}$ ,  $b'_{\text{PF}}$ ) of the symmetric type 2 solutions, at which they are stabilized, are plotted for  $N = 10$  (a solid line), 20 (a dashed line), 30 (a dotted line), and 40 (a dash-dotted line). The pitchfork bifurcation points ( $g_{\text{PF}}$ , 0.0) in the absence of the bias are also plotted with triangles. The values  $g'_{\text{PF}}$  at the pitchfork bifurcation points are shifted to smaller  $g$  as the bias  $b$  increases so the stabilization of the type 2 solutions occurs at smaller  $g$ . Further, the loci tend to be tangential to the line of  $b = 0$  for large  $N$  and then the stability of the type 2 solutions is sensitive to small biases. In Fig. 3, the values  $g'_{\text{PF}}$  at the pitchfork

bifurcation points of the symmetric type 2 solutions with  $b = 0.01$  are plotted with open triangles. The range of  $l_0$  in which the duration of spatially nonuniform patterns increases exponentially is restricted between the solid circles  $g_1$  (solid circles) and  $g'_{\text{PF}}$  (open triangles), where  $l_0 = N/2$ . When  $g = 1.1$ , for instance, the upper bound of  $l_0$  decreases to less than 15 ( $N = 30$  in Fig. 3) and actually  $l_0 = 14$  so the maximum duration becomes only  $10^3$  (see Fig. 5). The type 2 solutions are easily stabilized and an exponential increase in the duration of transient patterns is lost in the presence of such small biases in coupling strength.

## V. EFFECTS OF ASYMMETRY IN COUPLING

In this section, we consider effects of asymmetry in the direction of coupling in Eq. (1), i.e.,  $c_{n,n\pm 1}$  is constant but  $c_{n,n-1} \neq c_{n,n+1}$ . When the strengths of the forward ( $c_{n,n-1}$ ) and backward ( $c_{n,n+1}$ ) couplings differ from each other, an unstable traveling-wave solution rotating in a ring is generated through the Hopf bifurcation from the origin. The traveling-wave solution changes into an unstable steady solution, i.e., pinning occurs as the output gain increases, which is common in spatially discrete coupled systems [32]. In the presence of the unstable traveling wave, it is shown that the duration of transient rotating waves also increases exponentially with the number of neurons.

Let the coupling strength be

$$c_{n,n-1} = 1/2 + d, c_{n,n+1} = 1/2 - d \quad (1 \leq n \leq N, c_{n\pm N,n'\pm N} = c_{n,n'}). \quad (20)$$

Coupling becomes unidirectional ( $c_{n,n\pm 1} = 1, c_{n,n\mp 1} = 0$ ) when  $d = \pm 1/2$ , and we let  $d > 0$  without loss of generality. The eigenvalues  $\lambda_k$  of the Jacobian matrix  $A$  of Eq. (1) with Eq. (20) evaluated at the origin become complex values except for  $\lambda_0 (= -1 + g)$ .

$$\lambda_k = -1 + g[\cos(2k\pi/N) + i2d\sin(2k\pi/N)] \quad (0 \leq k < N). \quad (21)$$

A pair of stable spatially uniform steady solutions is first generated from the origin at  $g = g_0 = 1$  ( $k = 0$ ) and Eq. (1) becomes bistable. An unstable limit cycle is then generated through the Hopf bifurcation when the real part of a pair of complex conjugate eigenvalues,  $\lambda_1$  and  $\lambda_{N-1}$ , becomes positive at  $g = g_1 = 1/\cos(2\pi/N)$  when  $N \geq 5$ . This limit cycle is a traveling wave propagating in the direction of the ascending order of  $n$  ( $1 \rightarrow N$ ) and its spatial pattern is similar to that of a spatially nonuniform steady solution when  $d = 0$ .

The unstable traveling wave is then pinned as  $g$  increases further when  $d$  is small ( $d \sim 0.01$ ), i.e., its speed becomes zero (the period of the limit cycle diverges). It breaks up into a saddle-node loop (a heteroclinic cycle) and  $N$  pairs of unstable steady solutions are generated. They have the same form by shifts in  $n$ , and one is a type 2 ( $N$ : even) or type 1 ( $N$ : odd) solution while the other is a type 0 solution. Their bifurcations with  $g$  are qualitatively the same as those in symmetric coupling ( $d = 0$ ). The type 2 solution for even  $N$  is stabilized through a pitchfork bifurcation, while the other solutions are not bifurcated.

Figure 11(a) shows a bifurcation diagram in the  $g$ - $d$  plane, in which the loci of the pinning points ( $g_{\text{PIN}}$ ,  $d_{\text{PIN}}$ ) (a solid line)

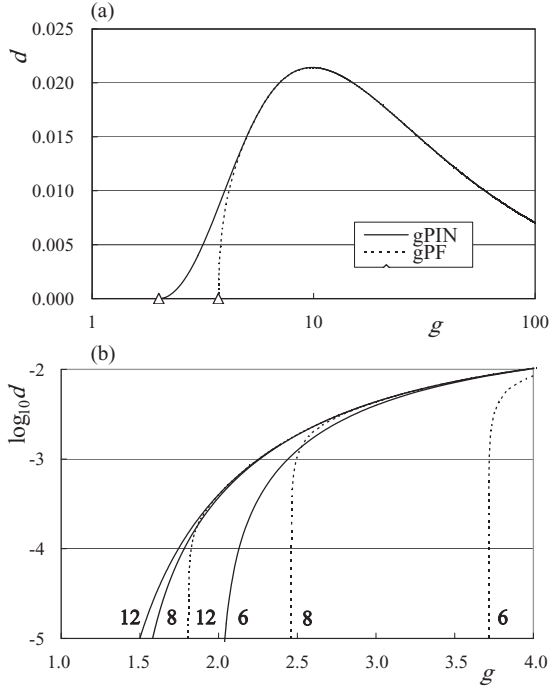


FIG. 11. Bifurcation diagram of Eqs. (1) and (20) in the  $g$ - $d$  plane. (a) Loci of the pinning points ( $g_{\text{PIN}}, d_{\text{PIN}}$ ) (a solid line) of the traveling wave and the pitchfork bifurcation points ( $g_{\text{PF}}, d_{\text{PF}}$ ) (a dotted line) of the type 2 solution, and ( $g_1, 0.0$ ), ( $g_{\text{PF}}, 0.0$ ) (triangles) for  $N = 6$ . (b) Magnification near  $d = 0$ . Loci of the pinning points ( $g_{\text{PIN}}, d_{\text{PIN}}$ ) (solid lines) and the pitchfork bifurcation points ( $g_{\text{PF}}, d_{\text{PF}}$ ) (dotted lines), and ( $g_1, 0.0$ ), ( $g_{\text{PF}}, 0.0$ ) (triangles) for  $N = 6, 8, 12$ .

of the traveling wave and the pitchfork bifurcation points ( $g_{\text{PF}}, d_{\text{PF}}$ ) (a dotted line) of the type 2 solution with  $N = 6$  are plotted. Note that the abscissa is scaled logarithmically. The locus of pinning points ( $g_{\text{PIN}}, d_{\text{PIN}}$ ) connects to the pitchfork bifurcation point [ $g_1 (=2.0), 0.0$ ] of the type 2 solution from the origin at  $d = 0.0$ , and the locus of the pitchfork bifurcation points ( $g_{\text{PF}}, d_{\text{PF}}$ ) connects to the corresponding one [ $g_{\text{PF}} (=3.72), 0.0$ ]. The two loci merge together as  $g$  increases ( $g > 5.0$ ). It can be shown that they hardly depend on the number  $N$  of neurons when  $g$  is large ( $g > 5.0$ ) and  $d_{\text{PIN}} = 1/g_{\text{PIN}}$  in the limit of  $g \rightarrow \infty$ , while they connect to the corresponding pitchfork bifurcation points [ $(g_1, 0.0)$ , ( $g_{\text{PF}}, 0.0$ )]. Figure 11(b) shows the loci of the pinning points (solid lines) and the pitchfork bifurcation points (dotted lines) in the  $g$ - $d$  plane for  $N = 6, 8$ , and 12. The number of neurons is indicated along each locus. As  $N$  increases, the separation of two loci is shifted to smaller  $g$  and, hence, to smaller  $d$ . The unstable traveling wave changes into a stable steady solution almost at the same time of pinning when  $N$  is large, unless  $d$  is extremely small.

Stable spatially asymmetric steady solutions [type  $2n$  ( $n \geq 1$ )] are also generated through saddle-node bifurcations in the same manner as symmetric coupling. It can be shown that these saddle-node bifurcation points change in the same manner in the  $g$ - $d$  plane as the pitchfork bifurcation point of the type 2 solution for even values of  $N$  in Fig. 11. Hence, the traveling wave is pinned and then a stable type 2 solution is generated through a saddle-node bifurcation as  $g$  increases when  $N$  is odd.

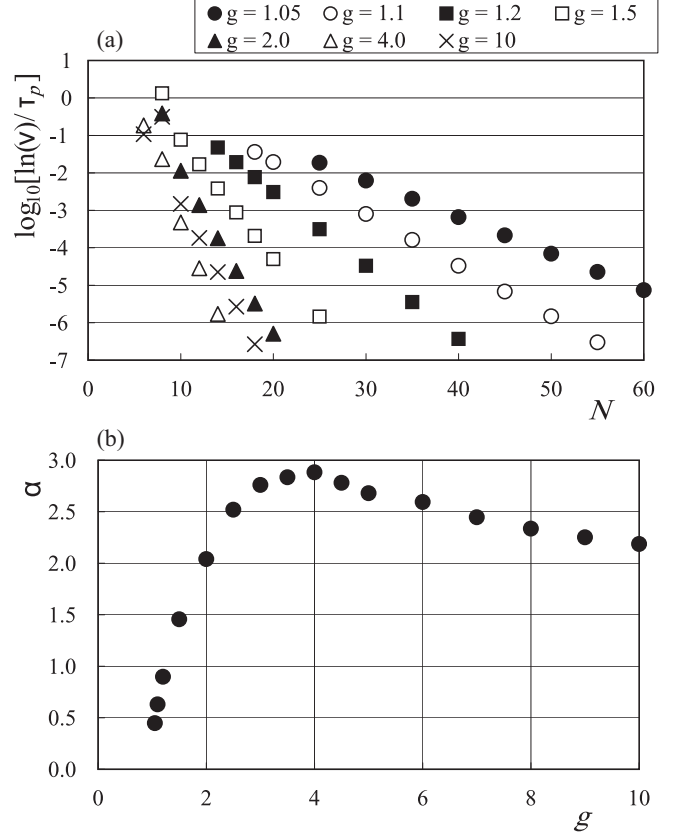


FIG. 12. (a) Semilog plot of  $\ln(v)/\tau_p$  of the traveling-wave solution vs the number  $N$  of neurons in Eqs. (1) and (20) with  $d = 0.1$  and  $g = 1.05$  (solid circles), 1.1 (open circles), 1.2 (solid squares), 1.5 (open squares), 2.0 (solid triangles), 4.0 (open triangles), and 10 (crosses).  $v$ : the largest eigenvalue of the Poincaré map;  $\tau_p$ : the period. (b) Estimated exponential growth rate  $\alpha$  in Eq. (12) vs the output gain  $g$ .

The traveling waves (not pinned) are always unstable, but their instability decreases exponentially with the number  $N$  of neurons in the same manner as the spatially nonuniform steady solutions for  $d = 0$ . A change in the bump width  $l$  in a transient state is described by the kinematical equations (6) and (10) [17]. The duration  $T$  of spatially asymmetric rotating waves with the initial width  $l_0$  of a smaller bump is then given by Eqs. (9) and (12). The coefficient  $2\alpha\beta\exp(-\alpha N/2)$  ( $=\mu$ ) of the perturbation  $l'$  ( $=l - N/2$ ) in Eq. (7) is estimated with  $\ln(v)/\tau_p$ , where  $v$  is the largest eigenvalue of the Poincaré map of the traveling-wave solution and  $\tau_p$  is its period. This estimate is derived as  $l'(\tau_p)/l'(0) = \exp[2\alpha\beta\exp(-\alpha N/2)\tau_p] = v$ . Figure 12(a) shows a semilog plot of  $\ln(v)/\tau_p$  of the traveling-wave solution against the number  $N$  of neurons in Eqs. (1) and (20) with  $d = 0.1$  and  $g = 1.05$  (solid circles), 1.1 (open circles), 1.2 (solid squares), 1.5 (open squares), 2.0 (solid triangles), 4.0 (open triangles), and 10 (crosses). The value of  $\ln(v)/\tau_p$  decreases exponentially with  $N$ ; hence, the relaxation time of the unstable traveling waves ( $\sim\tau_p/\ln(v)$ ) increases exponentially with  $N$ .

Figure 12(b) shows the exponential growth rate  $\alpha$  of the duration of spatially asymmetric rotating waves in Eq. (12) against the output gain  $g$  (solid circles). The values of  $\alpha$  were estimated with the slopes of the graphs of  $\ln(v)/\tau_p$  vs  $N$

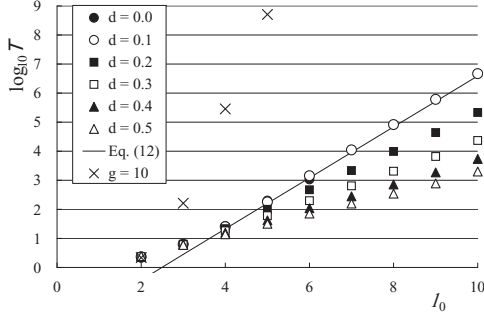


FIG. 13. Semilog plot of the duration  $T$  of spatially asymmetric rotating waves in Eqs. (1) and (20) vs the initial width  $l_0$  of a smaller bump. Results of computer simulation with  $N = 21$  under Eq. (13):  $g = 2.0$  and  $d = 0.0 - 0.5$  by 0.1 (circles, squares and triangles); Eq. (12) for  $g = 2.0$  and  $d = 0.1$  (a solid line);  $g = 10.0$  and  $d = 0.03$  (crosses).

in Fig. 12(a) [ $\ln(v)/\tau_p = 2\alpha\beta\exp(-\alpha N/2)$ ]. The growth rate increases for small  $g$  ( $1 < g < 3$ ) in a similar manner to that of the steady-state solutions for  $d = 0.0$  in Fig. 6, and it is slightly smaller than that in Fig. 6. However, its increase is saturated and it reaches its maximum ( $\approx 2.7$ ) at  $g \approx 3.5$  and then begins to decrease gradually. It has been shown that the growth rate  $\alpha$  of the duration of rotating waves hardly depends on  $g$  in a ring of unidirectionally coupled sigmoidal neurons ( $d = 1/2$ ) for  $g \geq 1.1$  [18]. This rate is approximated as  $\alpha = \ln 2$  ( $\approx 0.7$ ), which is derived in the limit of  $g \rightarrow \infty$ . The growth rate thus changes as  $d$  increases, since it depends on  $g$  as shown in Fig. 12(b).

Figure 13 shows a semilog plot of the duration  $T$  of spatially asymmetric rotating waves against the initial width  $l_0$  of a smaller bump with  $d = 0.0 - 0.5$  by 0.1. They were obtained by computer simulation of Eqs. (1) and (20) with  $N = 21$  and  $g = 2.0$  under the initial condition Eq. (13). The duration of the rotating waves increases exponentially with  $l_0$ , and the values for small  $d$  ( $=0.1$ ) (open circles) are about the same as those for  $d = 0.0$  (solid circles). The growth rate  $\alpha = 2.03$  for  $d = 0.1$  is slightly smaller than  $\alpha = 2.38$  for  $d = 0.0$ , as shown in Figs. 12(b) and 6, respectively. Although steady asymmetric patterns are stabilized for  $l_0 \geq 7$  when  $d = 0.0$  (Fig. 5), the traveling waves are not stabilized and their duration can increase to infinity with the initial bump width  $l_0$ . Equation (12) with  $\alpha = 2.04$  and  $\beta = 75.2$  estimated with the graph for  $g = 2.0$  in Fig. 12(b) agrees with the simulation results for  $d = 0.1$  (a solid line). As  $d$  increases from 0.1 to 0.5, the growth rate  $\alpha$  (the slope of the graph) decreases from 2.03 to 0.8 and approaches the constant value ( $\approx \ln 2$ ) as noted above. When  $g$  is large and  $d$  is close to  $d_{PIN}$  ( $\approx d_{PF}$ ), the growth rate becomes more than five, e.g.,  $\alpha = 7.5$  when  $g = 10$  and  $d = 0.03$  ( $> d_{PIN} = 0.0214$ ), which is plotted with crosses in Fig. 13. The traveling waves then become practically stable even though  $l_0$  is small.

## VI. EFFECTS OF ASYMMETRY IN THE OUTPUT FUNCTION

In this section, we consider the effects of asymmetry in the output function  $f$  of a neuron on transient states. When the  $\mathbf{Z}_2$

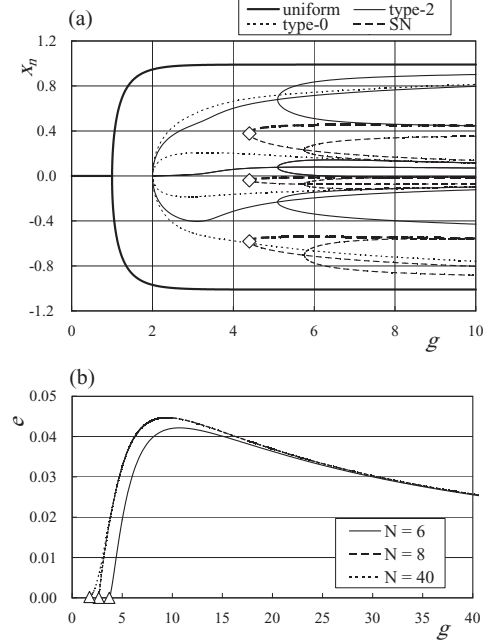


FIG. 14. Bifurcation diagram of Eqs. (1) and (22) with  $e = 0.01$ . (a) The states ( $x_n$ ,  $1 \leq n \leq N$ ) of all neurons vs the output gain  $g$  for  $N = 6$ . Stable solutions (thick lines), unstable solutions (thin lines), saddle-node bifurcation points ( $g_{SN}$ ,  $e_{SN}$ ) in the  $g$ - $e$  plane for  $N = 6$  (a solid line), 8 (a dashed line), and 40 (a dotted line), and the pitchfork bifurcation points ( $g_{PF}$ ,  $0.0$ ) (triangles).

symmetry of Eq. (1) is broken because of the asymmetry in  $f$ , the strength of the stability of a spatially uniform positive solution differs from that of a negative one. In a bistable reaction-diffusion equation, it is known that a stationary kink changes into a traveling kink when a cubic function becomes asymmetric. As a result, the duration of a pulse pattern (a pair of kink and antikink) becomes linear with respect to the pulse width. It has also been shown that asymmetry in the output function degrades an exponential increase in the duration of transient rotating waves in a ring of unidirectionally coupled neurons [18]. In the following, it is shown that an exponential decrease in the largest eigenvalue of the Jacobian matrix  $A$  of Eq. (1) evaluated at the type 2 solution is lost so metastable dynamical transient patterns disappear.

The following asymmetric function  $f_e$  is used instead of  $f(x) = \tanh(x)$  in Eq. (1):

$$f_e(x) = [1 - \exp(-2x)] / [(1 + e) + (1 - e)\exp(-2x)]. \quad (22)$$

Note that  $f_e(x) = \tanh(x)$  when  $e = 0$ . The asymptotic values at infinity of  $x$  are shifted from  $\pm 1$  as  $f_e(x) \rightarrow 1/(1 + e)$  ( $x \rightarrow \infty$ ),  $f_e(x) \rightarrow -1/(1 - e)$  ( $x \rightarrow -\infty$ ). Since we can let  $f_e(x) \rightarrow -f_e(-x)$  and  $x \rightarrow -x$  when  $e \rightarrow -e$ , we let  $e > 0$  without loss of generality. The asymptotic values  $f_e(\infty)$  and  $f_e(-\infty)$  then decrease from  $\pm 1$  by  $e/(1 + e)$  and  $e/(1 - e)$ , respectively. We here consider symmetric bidirectional coupling and use Eq. (2). The origin is a steady solution and the eigenvalues of the Jacobian matrix  $A$  evaluated at the origin are the same as in Eq. (4), since  $f_e'(0) = f'(0) = 1$ .

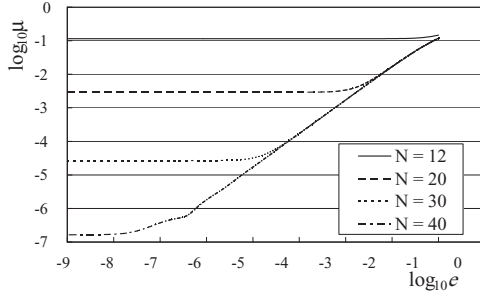


FIG. 15. Log-log plot of the largest eigenvalue  $\mu$  of the Jacobian matrix  $A$  evaluated at the solution of Eqs. (1) and (22) corresponding to the type 2 solution vs  $e$  when  $g = 1.2$  and  $N = 12$  (a solid line), 20 (a dashed line), 30 (a dotted line), and 40 (a dash-dotted line).

Figure 14(a) shows a bifurcation diagram of Eqs. (1) and (22) with  $e = 0.01$  and  $N = 6$ , in which the states  $(x_n, 1 \leq n \leq N)$  of all neurons are plotted against the output gain  $g$ . The branches of stable (unstable) solutions are plotted with thick (thin) lines. The first bifurcation of the origin at  $g = g_0 (=1)$  becomes transcritical, although it is scarcely visible. The branch of a generated stable spatially uniform solution with neurons of positive states reaches  $g = 10$ , and that of an unstable solution with neurons of negative states is quickly stabilized through a saddle-node bifurcation ( $g = 0.99993$ ) and turns to reach  $g = 10$  (thick solid lines). Two pairs of unstable spatially nonuniform steady solutions [type 2 (thin solid lines), type 0 (thin dashed lines)] are also generated through a degenerate pitchfork bifurcation due to the  $D_n$  symmetry from the origin at  $g = g_1 (=2.0)$ . The states of neurons in these solutions are shifted to positive from those for  $e = 0.0$ , e.g., the values of the zero-state neurons of the type 2 solution become positive. They correspond to the boundaries of the basins of the stable spatially uniform solutions and they are shifted to a positive solution with a weak stability and a small basin. A stable spatially nonuniform solution (thick dashed lines) is generated through a saddle-node bifurcation at  $g = g_{SN} = 4.40$  (diamonds), even though the value of  $N$  is even because of the breaking of the  $Z_2$  symmetry. The states of neurons in the stable solution are shifted to negative from the type 2 solution for  $e = 0.0$ .

Figure 14(b) shows a bifurcation diagram in the  $g$ - $e$  plane, in which the loci of the saddle-node bifurcation points ( $g_{SN}$ ,  $e_{SN}$ ) of the stable spatially nonuniform steady solutions for  $N = 6$  (a solid line), 8 (a dashed line), and 40 (a dotted line) are plotted. They connect to the pitchfork bifurcation points (e.g.,  $g_{PF} = 3.72$  for  $N = 6$ ) of the symmetric type 2 solutions at  $e = 0.0$  (triangles). The loci for  $N \geq 8$  are almost the same except for  $e \approx 0.0$ . The stable spatially nonuniform solutions exist in the regions under the loci.

Figure 15 shows a log-log plot of the largest eigenvalue  $\mu$  of the Jacobian matrix  $A$  [Eq. (3)] evaluated at the solution of Eqs. (1) and (22) generated from the origin corresponding to the unstable symmetric type 2 solution against  $e$  when  $g = 1.2$  and  $N = 12$  (a solid line), 20 (a dashed line), 30 (a dotted line), or 40 (a dash-dotted line). The largest eigenvalue  $\mu$  begins to increase when  $e$  reaches approximately the value of  $\mu$  at  $e = 0.0$ , and then the two terms take approximately the same value ( $\mu \approx e$ ). The eigenvalues smaller than the value

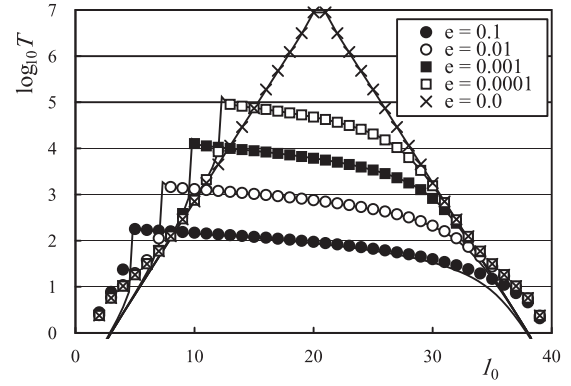


FIG. 16. Semilog plot of the duration  $T$  of spatially nonuniform patterns in Eqs. (1) and (22) vs the initial width  $l_0$  of a smaller bump. Results of computer simulation with  $g = 1.2$  and  $N = 40$  under Eq. (13) for  $e = 0.1$  (solid circles), 0.01 (open circles), 0.001 (solid squares), 0.0001 (open squares), and 0.0 (crosses). Solutions to Eq. (23) ( $e > 0$ ) and Eq. (9) ( $e = 0$ ) (solid lines).

of  $e$  thus disappear even for large  $N$ , and the maximum of the duration of spatially nonuniform patterns decreases until it is on the order of  $1/e$ .

Figure 16 shows a semilog plot of the duration  $T$  of spatially nonuniform patterns against the initial width  $l_0$  of a smaller bump, which was obtained with computer simulation of Eqs. (1) and (22) with  $g = 1.2$  and  $N = 40$  under the initial condition Eq. (13). Plotted are the values for  $e = 0.1$  (solid circles), 0.01 (open circles), 0.001 (solid squares), 0.0001 (open squares), and 0.0 (crosses). The exponential increase in the duration with  $l_0$  degrades and its increase is actually linear with respect to  $l_0$ .

This change in the duration of transient patterns due to the asymmetry  $e$  is explained by adding a small constant  $\gamma$  to the kinematical equations (6) and (10),

$$\begin{aligned} dl/dt &= \gamma + \beta \{ \exp[-\alpha(N-l)] - \exp(-\alpha l) \} \quad (0 < l < N) \\ &\approx \gamma - \beta \exp(-\alpha l) \quad (0 < l < N/2). \end{aligned} \quad (23)$$

The constant  $\gamma$  corresponds to double the speed of a traveling kink solution propagating in an infinite linear chain of neurons. Equation (23) can be solved and the duration  $T$  of spatially nonuniform patterns has the following form [18,33]:

$$\begin{aligned} T &\approx [\exp(\alpha l_0) - 1]/(\alpha\beta) \quad (0 < l_0 < l_c) \\ &\approx (N - l_0)/\gamma \quad (l_c < l_0 < N - l_c) \\ &\approx [\exp(\alpha(N - l_0)) - 1]/(\alpha\beta) \quad (N - l_c < l_0 < N) \\ (l_c &\approx \log(\beta/\gamma)/\alpha). \end{aligned} \quad (24)$$

A change in  $T$  for  $l_c < l_0 < N - l_c$  becomes linear to  $l_0$ . An exponential increase in  $T$  around  $N/2$  then disappears and the maximum of  $T$  is about  $(N - l_c)/\gamma$ . The threshold width  $l_c$  decreases as  $\gamma$  increases, and the regions  $(0 < l_0 < l_c, N - l_c < l_0 < N)$  for the exponential increase in  $T$  become small. The solutions to Eq. (23) ( $e > 0$ ) and Eq. (9) ( $e = 0$ ) are also plotted with solid lines in Fig. 16. Since the value of  $\gamma$  cannot be obtained analytically, we estimated it experimentally as  $\gamma = 1.83e$ . These lines agree with the simulation results except in the case of  $l_0 \approx 0$  and  $l_0 \approx N$ .

The graphs of duration  $T$  in Fig. 9 have similar forms unless spatially nonuniform patterns are stabilized, in which case random variations in coupling strength are added. Randomness in coupling strength can cause biases equivalent to the asymmetry in the output function, e.g.,  $c_{n,n-1} < c_{n,n+1}$  for  $1 \leq n \leq N/2$  and  $c_{n,n-1} > c_{n,n+1}$  for  $N/2 + 1 \leq n \leq N$ . Random variations in coupling strength thus also tend to degrade an exponential increase in the duration of transient patterns in addition to causing the stabilization of spatially nonuniform patterns. Since the intrinsic coupling strength in the framework of Eq. (1) is  $c_{n,n'}g$ , the stabilization of spatially nonuniform patterns can be caused by adding the bias  $e$  randomly to the output function of each neuron.

### VII. TRANSIENT PATTERNS IN A TWO-DIMENSIONAL ARRAY

In this section, we study the duration of transient patterns in a two-dimensional array of sigmoidal neurons with symmetric nearest-neighbor coupling. The model equation is

$$\begin{aligned} dx_{m,n}/dt &= -x_{m,n} + [f(gx_{m-1,n}) + f(gx_{m+1,n}) \\ &\quad + f(gx_{m,n-1}) + f(gx_{m,n+1})]/4 \\ f(x) &= \tanh(x) (1 \leq m \leq M, 1 \leq n \leq N, \\ x_{m \pm M,n} &= x_{m,n \pm N} = x_{m,n}), \end{aligned} \quad (25)$$

where a periodic boundary condition is imposed. Equation (25) has a pair of stable spatially uniform steady solutions:  $x_{m,n} = \pm x_s$  ( $1 \leq m \leq M$ ,  $1 \leq n \leq N$ ) with  $x_s = \tanh(gx_s)$  when  $g > 1$ . It also has steady solutions with the one-dimensional forms, in which the states of neurons depend only on  $n$ :  $x_{m,n} = x_n$  ( $1 \leq m \leq M$ ,  $1 \leq n \leq N$ ). These solutions are obtained by the following equation for a ring of bidirectionally coupled neurons.

$$\begin{aligned} dx_n/dt &= -x_n + [f(gx_{n-1}) + f(gx_{n+1})]/2 + f(gx_n)/2 \\ f(x) &= \tanh(x) (1 \leq n \leq N, x_{n \pm N} = x_n). \end{aligned} \quad (26)$$

In contrast to the case of diffusive coupling, a term of self-excitation [ $f(gx_n)/2$ ] through two adjacent neurons in the direction of  $m$  is added. The eigenvalues  $\lambda'_k$  of the Jacobian matrix evaluated at the origin of Eq. (26) are given by

$$\lambda'_k = -1 + g[1 + \cos(2k\pi/N)]/2 \quad (0 \leq k < N). \quad (27)$$

Unstable spatially nonuniform steady solutions to Eq. (26) are generated through pitchfork bifurcations from the origin when the values of  $\lambda'_k$  ( $k \geq 1$ ) become zero as  $g$  increases when  $N \geq 3$ . The values of  $g'_k = 2/[1 + \cos(2k\pi/N)]$  ( $k \geq 1$ ) at the pitchfork bifurcation points are smaller than those [ $g_k = 1/\cos(2k\pi/N)$ ] of Eq. (1). These solutions are also stabilized at smaller values of  $g$  than those of Eq. (1) when  $N$  is even. Pairs of stable and unstable asymmetric steady solutions are also generated through saddle-node bifurcations. In contrast to Eq. (1), stable solutions are not type 2 but type 0, i.e., they have no zero-state neurons [ $x_n \neq 0$  ( $1 \leq n \leq N$ )], which is due to self-excitation. Actually, it can be shown that the stabilities of type 0 and type 2 solutions are interchanged through successive pitchfork bifurcations as the strength of self-excitation increases.

The largest eigenvalues of the spatially nonuniform solutions generated from the origin also decrease exponentially

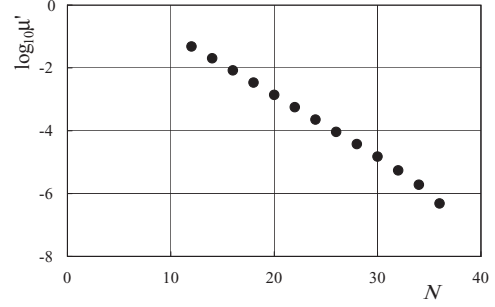


FIG. 17. Semilog plot of the largest eigenvalue  $\mu'$  of the Jacobian matrix evaluated at the unstable type 0 solution of Eq. (26) with  $g = 1.1$  vs the number  $N$  of neurons.

with  $N$  when  $g$  is small enough that they are not stabilized when  $N$  is even and that stable spatially nonuniform solutions are not generated when  $N$  is odd. Figure 17 shows a semilog plot of the largest eigenvalue  $\mu'$  of the Jacobian matrix of Eq. (26) evaluated at the unstable type 0 solution against the number  $N$  of neurons at  $g = 1.1$ . The solution is stabilized at  $N = 38$ , which is smaller than that in Eq. (1) ( $N$  at the stabilization is more than 60), but the slope of the graph in the unstable region is larger than that of Eq. (1) in Fig. 4. As a result, the values of the smallest eigenvalues are in the same order ( $\sim 10^{-6}$ ). The kinematical equations (6) and (10) can also be applied for spatially nonuniform patterns and the values of the parameters  $\alpha$  and  $\beta$  can be estimated from the graph of  $\mu'$  vs  $N$  in Fig. 17. The duration of spatially nonuniform patterns in Eq. (26) also increases exponentially with the initial width of a smaller bump.

In a two-dimensional array of neurons [Eq. (25)], these solutions with the one-dimensional forms are first generated as  $g$  increases before solutions with various shapes are generated. In computer simulation, solutions with patterns other than one-dimensional forms, e.g., bounded island patterns, are generated through saddle-node bifurcations at large  $g$ , e.g.,  $g > 6$  when  $M = N = 20$ . Further, when the initial values of  $x_{m,n}$  are given randomly, the array is quickly separated into domains consisting of neurons with positive and negative states as a bistable reaction-diffusion equation in a two-dimensional domain. It is known that the motion of the boundaries of domains depends on their curvature [2,3]. If the same kinematics is applicable to an array of neurons, patterns with nonzero curvature disappear more quickly than patterns with zero curvature when there are no stable solutions other than a pair of spatially uniform solutions. It is thus expected that only metastable dynamical patterns with the one-dimensional forms remain for a long time and become dominant in transients, in which the motion of the boundaries is exponentially slow.

Figure 18 shows a log-log plot of a normalized histogram of the duration  $T$  obtained with 1000 runs of computer simulation of Eq. (25) with  $g = 1.1$  and  $M = N = 35$  under a random Gaussian initial condition:  $x_{m,n}(0) \sim N(0, 0.1^2)$  ( $1 \leq m, n \leq N$ ) (solid circles). Equations (15) and (16) with  $N = 35$ ,  $\alpha = 0.92$ , and  $\beta = 14.5$  estimated from Fig. 17 are also plotted with solid and dashed lines, respectively, where the cut-off is  $T_c = 7.4 \times 10^5$ . These results agree with the simulation result, and thus the duration of transient patterns depends not on the total number ( $M \times N$ ) of neurons in an array but

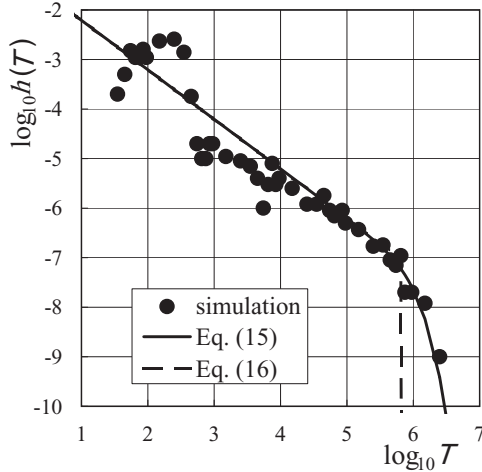


FIG. 18. Log-log plot of a normalized histogram of the duration  $T$  obtained with 1000 runs of computer simulation of Eq. (25) with  $g = 1.1$  and  $M = N = 35$  under a random Gaussian initial condition:  $x_{m,n}(0) \sim N(0, 0.1^2)$  ( $1 \leq m, n \leq N$ ) (solid circles). Equations (15) (a solid line) and (16) (a dashed line) with  $N = 35$ ,  $\alpha = 0.92$ , and  $\beta = 14.5$ .

rather on the number  $[\min(M, N)]$  of neurons within a single row of an array. Metastable dynamical patterns emerging in a two-dimensional array of neurons are intrinsically dominated by one-dimensional dynamics.

### VIII. DISCUSSION

We examined a ring network consisting of simple sigmoidal neuron models to study its bifurcations and show metastable dynamical transient patterns. As mentioned in Sec. I, however, metastable dynamical transient rotating waves in the form of propagating oscillations have been found in a ring of unidirectionally coupled Bonhoeffer-van der Pol neuron models with slow inhibitory synapses [25]. The results obtained in this paper are applicable to such networks consisting of biologically plausible spiking neurons with inhibitory bidirectional coupling. Positive and negative output of a sigmoidal neuron correspond to the firing and resting states of a spiking neuron, respectively. Firing neurons and resting neurons are alternately located in the steady states of a ring of inhibitorily coupled spiking neurons. In transients, there are two inconsistencies at which adjacent neurons are in the same state (firing-firing or resting-resting) and their locations move in the direction of coupling. Although we dealt with a ring of neurons with excitatory coupling ( $c_{n,n'} > 0$ ), the excitatory ring can be changed into a ring with inhibitory coupling if the number of neurons is even. That is, these two types of coupling can be interchanged by changing the signs of neurons states to even (or odd) indices [ $x_{2m} \rightarrow -x_{2m}$  ( $1 \leq m \leq N/2$ )] when the strength of coupling is constant ( $c_{n,n'} = c$ ). Analysis of the bifurcations and stability of propagating oscillations is difficult because the waves are quasiperiodic and they take the form of changes in the locations of the inconsistencies, not changes in the states of individual neurons. Thus, the findings in this paper are useful in examining conditions for the emergence of metastable dynamical firing patterns of spiking neurons.

First, it was shown in Sec. II that spatially nonuniform steady solutions are stabilized in a ring of a small number of neurons when the output gain of the neuron is large ( $g \gg 1$ ). Long-lasting transient patterns in a ring of a large number of neurons existed only in the case of small output gains ( $g \approx 1$ ). This result indicates that metastable dynamical transient nonpropagating firing patterns emerge in rings of bidirectionally coupled spiking neurons that show graded responses. It is known that the firing activity of neurons can be classified into two types according to their responses to a constant current [34]. A class I neuron is capable of repetitive firing over a wide range of frequencies, which varies smoothly with the strength of the applied current. A class II neuron fires in a limited range of frequencies, which is relatively insensitive to changes in current strength. In a mathematical context, the transitions between resting state and firing state occur in response to homoclinic bifurcations in class I neurons and subcritical Hopf bifurcations in class II neurons. Thus, a class I neuron can fire with zero (arbitrarily low) frequency while a class II neuron begins to fire with a characteristic nonzero frequency when the strength of the current crosses a threshold. It is thus more likely that metastable dynamical transient patterns will appear in rings of bidirectionally coupled class I neurons than in class II neurons. It is of interest to study the metastable dynamical transient firing patterns in rings of bidirectionally coupled class I neuron models, e.g., the Morris-Lecar model [35] and the Hindmarsh-Rose model [36]. An integrate-and-fire model is also regarded as a simple and more tractable model of a class I neuron [37]. It is hoped that metastable dynamics will be able to be analytically investigated through networks of coupled integrate-and-fire neuron models.

Section V showed that traveling waves generated in the presence of asymmetry in bidirectional coupling are unstable even when they are nearly pinned. The nearly pinned rotating waves showed metastable dynamics and the duration of the transient rotating waves was extremely long even in rings with small numbers of neurons ( $l_0 = 5$  in Fig. 13). Such long-lasting propagating oscillations might be observed in rings of small numbers of spiking neurons with asymmetric bidirectional coupling.

In Sec. VI, asymmetry in the sigmoidal output function of a neuron degraded an exponential increase in the duration of the transient patterns. The two states (firing and resting) of a spiking neuron qualitatively differ from each other and thus the output of neurons is regarded as asymmetric. This is probably the reason why metastable dynamical propagating oscillations have been observed in a ring of spiking neurons coupled through inhibition, not excitation. Bifurcation analysis and computer simulation can show that the metastable dynamics of rotating waves remains in the presence of large asymmetry in the sigmoidal output function when the coupling is inhibitory. In Sec. IV, it was also shown that random variations in the strength of coupling (also random biases in the output functions of neurons) have considerable effects on metastable dynamical patterns. The variations stabilized spatially nonuniform patterns or degraded an exponential increase in their duration. However, it has been shown that the effects of variations and biases are suppressed to some extent in circuit experiments with ICs on metastable dynamical

propagating waves when coupling is inhibitory (negative) [17,38]. These findings support the possibility that metastable dynamical transient nonpropagating oscillations exist in rings of inhibitorily coupled spiking neurons. They might also emerge in open chains and two-dimensional arrays of spiking neurons, as shown in Appendix B and Sec. VII, respectively.

Although it is believed that metastable dynamics commonly emerges in systems with symmetric bistability, it is meaningful to show that they are realized in coupled dynamical systems consisting of elements showing complicated behaviors like neurons. In addition, metastable dynamical rotating waves have been found in bistable rings of coupled maps [39]. Since a discrete time map is regarded as the Poincaré map in a continuous time system, this finding indicates that metastable dynamical transients exist in systems which have bistable periodic solutions. In fact, it has been shown that the duration of transient propagating phase waves in a ring of unidirectionally coupled parametric oscillators increases exponentially with the number of oscillators [40]. Such systems of coupled parametric oscillators arise in microelectromechanical systems (MEMS), which are widely used as sensors of various kinds and many other devices. Hence, their analysis is of practical importance in mechanical and electronic engineering. In contrast to a neuron, a single parametric oscillator has a couple of stable periodic oscillations with a phase difference  $\pi$ , i.e., the oscillator is symmetrically bistable in itself without coupling or input. Bidirectional coupling is then simply diffusive, due to the mechanical or electric resistance intrinsic to the materials. Thus, metastable dynamical nonpropagating spatially nonuniform phase patterns might emerge under natural physical conditions.

## IX. CONCLUSION AND FUTURE WORK

In this paper, metastable dynamical patterns and their stabilization in a ring of bidirectionally coupled sigmoidal neurons were studied. First, the generation and bifurcations of steady solutions to the system were shown. A pair of stable spatially uniform solutions was generated from the origin and pairs of unstable spatially nonuniform solutions were generated successively as the output gain increased. A further increase in the output gain caused the stabilization of the spatially nonuniform solutions through a pitchfork bifurcation when the number  $N$  of neurons was even and caused the generation of a stable spatially nonuniform solution through a saddle-node bifurcation when  $N$  was odd. When the system was bistable, the largest eigenvalues of the unstable spatially nonuniform solutions decreased exponentially with the number of neurons. As a result, transient patterns showed metastable dynamics: The duration of spatially nonuniform patterns increased exponentially with the initial width of a smaller bump, and the distribution of the duration of randomly generated patterns obeyed a power-law distribution. The expression derived with a kinematical equation for a change in the bump width agreed with the simulation results.

Further, we showed the following: Small variations in coupling strength tend to stabilize spatially nonuniform patterns; asymmetry in the direction of coupling causes traveling waves and their pinning; and asymmetry in the output function degrades the exponential increase in the duration of transient

patterns. Finally, we considered a two-dimensional array of symmetrically coupled sigmoidal neurons and showed the solutions with the one-dimensional forms and a power-law distribution of the duration of randomly generated patterns.

There are four future areas of interest. The first is the effect of spatiotemporal noise. It is expected that spatiotemporal noise of intermediate intensity will increase the duration of spatially asymmetric patterns in the same manner as a ring of unidirectionally coupled sigmoidal neurons [18] and a bistable reaction-diffusion equation [33].

The second concerns the rotating waves in a ring of asymmetrically coupled neurons. A kinematics of unstable rotating waves in a ring of asymmetrically coupled neurons with large output gains can be derived. An increase in the growth rate of the duration of transient rotating waves near a pinning point, which is mentioned in Sec. V, can then be explained. Further, a power-law distribution of the duration of randomly generated rotating waves may appear even in rings of small numbers of neurons.

The third area of interest is inhibitory (negative) coupling. When coupling is inhibitory ( $c < 0$ ), the bifurcations and stability of solutions differ when the output function of a neuron is asymmetric and it is expected that metastable dynamical transient patterns remain. Further, when coupling is inhibitory and the number of neurons is odd, stable oscillations accompanying the generation of stable traveling waves occur (a ring oscillator). Pinning of these waves can occur in the presence of asymmetry in coupling.

The fourth area involves the effects of the self-excitation and self-inhibition of neurons. The growth rate of an exponential increase in the duration of transient patterns depends on the strength of self-excitation as shown in Sec. VII. It is expected that self-inhibition makes spatially nonuniform solutions unstable for larger output gains, and then the maximum duration of transient patterns increases.

## ACKNOWLEDGMENT

The author acknowledges valuable discussions with H. Kitajima.

## APPENDIX A: DURATION OF TRANSIENT PATTERNS IN CNN

The results of computer simulation on the duration of spatially nonuniform patterns in a one-dimensional cellular neural network (CNN) with a piecewise linear output function and symmetric coupling are shown. The model equation is

$$\begin{aligned} dx_n/dt &= -x_n + sf_L(x_{n-1}) + pf_L(gx_n) + sf_L(gx_{n+1}) \\ f_L(x) &= (|x+1| + |x-1|)/2 \quad (1 \leq n \leq N, x_{n \pm N} = x_n), \end{aligned} \quad (\text{A1})$$

where  $x_n$  is the state of the  $n$ th cell,  $s$  ( $>0$ ) is the strength of coupling with nearest-neighbor cells,  $p$  is the strength of self-coupling, and a periodic boundary condition is imposed. The origin is a steady solution to Eq. (A1) and the eigenvalues of the Jacobian matrix evaluated at the origin are given by

$$\lambda_k = p - 1 + 2s \cos(2k\pi/N) \quad (0 \leq k < N). \quad (\text{A2})$$

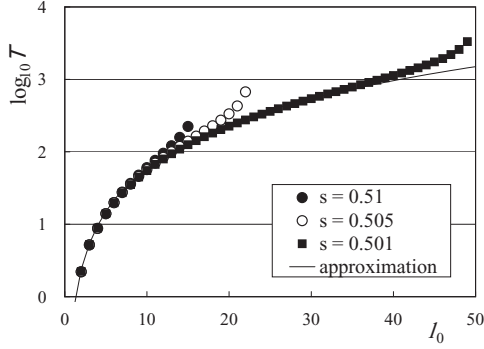


FIG. 19. Semilog plot of the duration  $T$  of spatially nonuniform patterns in Eq. (A1) vs the initial width  $l_0$  of a smaller bump. Results of computer simulation of Eq. (A1) with  $N = 100$ ,  $p = 0$  and  $s = 0.51$  (solid circles),  $0.505$  (open circles), and  $0.501$  (solid squares) under Eq. (13). Approximation:  $T = 0.6l_0^2$  (a solid line).

The origin is unstable when  $s > (1 - p)/2$  ( $\lambda_0 > 0$ ) and Eq. (A1) has a pair of spatially uniform steady solutions:  $x_n = \pm(p + 2s)$  ( $1 \leq n \leq N$ ). It has been shown that Eq. (A1) has a stable spatially nonuniform steady solution when  $s > (1 - p)/[2\cos(\pi/(B + 2))]$ , where  $N \geq 2(B + 2)$  and  $B$  is a nonnegative integer ( $B \geq 0$ ) [22]. The solution consists of a succession of at least two positively saturated cells [ $f_L(x_n) = 1$ ], a succession of at least two negatively saturated cells [ $f_L(x_n) = -1$ ] and two successions of  $B$  unsaturated cells [ $|f_L(x_n)| < 1$ ] connecting them. Conversely speaking, Eq. (A1) has no spatially nonuniform solution when  $N < 2(B + 2)$  with  $B < \pi/\arccos[(1 - p)/(2s)] - 2$ . Spatially nonuniform solutions are thus stable if they exist. There are no unstable spatially nonuniform solutions, the instability of which decreases exponentially with the number of cells as in those of Eq. (1). Consequently an exponential increase in the duration of transient patterns until convergence to one of the stable spatially uniform solutions does not emerge.

Figure 19 shows a semilog plot of the duration  $T$  of spatially nonuniform patterns against the initial width  $l_0$  of a smaller bump, which was obtained with computer simulation of Eq. (A1) with  $N = 100$ ,  $p = 0$ , and  $s = 0.51$  (solid circles),  $0.505$  (open circles), and  $0.501$  (solid squares) under the initial condition given in Eq. (13). The value of the duration  $T$  was obtained as a time at which the signs of the states of all cells became the same. The initial patterns converged stable spatially nonuniform solutions when  $l_0 > 15$  ( $s = 0.51$ ),  $l_0 > 22$  ( $s = 0.505$ ), and  $l_0 > 49$  ( $s = 0.501$ ). Approximation by a quadratic function,  $T = 0.6l_0^2$ , is also plotted with a solid line. The approximation agrees with the simulation results except when the values of  $l_0$  are close to the stabilization points, and thus the duration increases in proportion to the square of the initial width  $l_0$ . This quadratic relation reflects the strength of the stability of the origin with  $N = l_0 - 1$  under the Dirichlet boundary condition ( $x_0 = x_{l_0} = 0$ ), in which the largest eigenvalue of the Jacobian matrix evaluated at the origin is  $\lambda_{l_0} = p - 1 + 2s\cos(\pi/l_0) \approx -s(\pi/l_0)^2$  ( $p - 1 + 2s \approx 0$ ). That is, the states of cells first approach the origin and then approach one of the stable steady states  $\pm(p + 2s)$ . The duration of transient patterns obtained

with computer simulation thus corresponds to the convergence time ( $\sim 1/\lambda_{l_0}$ ) to the origin.

## APPENDIX B: BIFURCATIONS AND METASTABLE DYNAMICAL PATTERNS IN OPEN CHAINS OF NEURONS

Bifurcations and transient patterns in open chains of bidirectionally coupled sigmoidal neurons under Dirichlet and Neumann boundary conditions are considered. Solutions generated from the origin are restricted compared with those in a ring of neurons (a chain under a periodic boundary condition). Metastable dynamical spatially asymmetric patterns still exist when coupling is symmetric but disappear when coupling is asymmetric.

When a Dirichlet (absorbing) boundary condition ( $x_0 = x_{N+1} = 0$ ) is imposed, the eigenvalues of the Jacobian matrix evaluated at the origin in Eqs. (1) and (2) are given by  $\lambda_k = -1 + g\cos[k\pi/(N + 1)]$  ( $1 \leq k \leq N$ ). All eigenvalues are then simple and the corresponding pitchfork bifurcations at the origin are nondegenerate. Spatially nonuniform solutions with  $1 \leq k \leq N/2$  are generated as  $g$  increases through pitchfork bifurcations from the origin in a chain of  $N$  neurons. They are the same as the states  $x_n$  ( $1 \leq n \leq N$ ) of  $N$  neurons in the solutions with  $1 \leq k \leq N/2$  having at least two zero-state neurons ( $x_{N+1} = x_{2(N+1)} = 0$ ) generated from the origin in a ring of  $2(N + 1)$  neurons, in which  $x_n = (-1)^k x_{N+n}$  ( $1 \leq n \leq N$ ). A pair of stable spatially uniform solutions generated at  $g = g_0$  ( $=1.0$ ) in a ring of neurons is replaced by a pair of stable spatially nonuniform solutions generated at  $g = g_1$  with one bump patterns, i.e., one positive or negative bump in the spatially nonuniform solution with  $k = 1$  in a ring of  $2(N + 1)$  neurons. When  $N = (3 + m)k - 1$  ( $m$ : nonnegative integer), i.e.,  $(N + 1)/k$  is an integer with a value of 3 or more, the solution with the wave number  $k$  can be stabilized through pitchfork or transcritical bifurcations  $k - 1$  times as  $g$  increases. They have  $k - 1$  zero-state neurons and  $k$  bumps consisting of the same number ( $2 + m$ ) of neurons, and the states of neurons are  $(-1)^k x_{n+k'(3+m)}$  ( $1 \leq n \leq 2 + m$ ,  $0 \leq k' \leq k - 1$ ) with  $x_{k'(3+m)} = 0$  ( $1 \leq k' \leq k - 1$ ). The values of  $g$  at the bifurcations are also the same as those of the type  $2k$  solutions in a ring of  $2(N + 1)$  neurons, and the stabilization occurs for smaller  $g$  at the bifurcation earlier by one step. In the limit of  $g \rightarrow \infty$ , the states of neurons are  $\{(-1/2, -1 \times m, -1/2), [0, (-1)^k(1/2, 1 \times m, 1/2)] \times (k - 1)\}$ , where  $\times m$  and  $\times (k - 1)$  mean  $m$  and  $k - 1$  successions of the left elements, respectively. Stable spatially asymmetric solutions with a smaller bump consisting of at least two nonzero state neurons are also generated through saddle-node bifurcations with unstable ones when  $N \geq 6$ . The values of  $g$  at the saddle-node bifurcations depend almost entirely on the width of a smaller bump and are about the same as those in a ring of neurons, e.g.,  $g_{SN} = 3.63$  when the bump width is two.

When a Neumann (reflecting) boundary condition ( $x_0 = x_1$ ,  $x_{N+1} = x_N$ ) is imposed, the eigenvalues of the Jacobian matrix at the origin are given by  $\lambda_k = -1 + g\cos(k\pi/N)$  ( $0 \leq k \leq N - 1$ ), which are also simple. Spatially nonuniform solutions with  $0 \leq k \leq (N - 1)/2$  are generated through pitchfork bifurcations from the origin in a chain of  $N$  neurons. They are the same as the states  $x_n$  ( $1 \leq n \leq N$ ) of half of the neurons

in the solutions with  $0 \leq k \leq (N - 1)/2$  generated from the origin in a ring of  $2N$  neurons, in which the states of neurons are symmetric with respect to reflection at  $n = N + 1/2$ :  $x_{N+n} = x_{N-n+1}$  ( $1 \leq n \leq N$ ) and two bumps with the centers at  $n = 1/2$  and  $N + 1/2$  ( $x_0 = x_N$ ) consist of an even number of nonzero state neurons. When  $N = (3 + 2m)k$  ( $m$ : nonnegative integer), i.e.,  $N/k$  is odd and three or more, the  $k$ th solution can be stabilized through pitchfork or transcritical bifurcations  $k$  times as  $g$  increases. The states of neurons in the stabilized solutions and the values of  $g$  at the bifurcations are the same as the type  $2k$  solutions with the wave number  $k$  in a ring of  $2N$  neurons. They consist of  $k$  reflections of  $3 + 2m$  neurons with a zero-state neuron at the center [ $x_{2+m} = 0$ ,  $x_{2+m+n'} = -x_{2+m-n'}$  ( $1 \leq n' \leq m + 1$ )]. They have  $k$  zero-state neurons with  $k - 1$  and two halves of bumps consisting of the same number  $2(1 + m)$  of neurons. In the limit of  $g \rightarrow \infty$ , the states of neurons are  $[(-1)^k(1 \times m, 1/2, 0, -1/2, -1 \times m)] \times k$ , where  $\times m$  and  $\times k$  mean  $m$  and  $k$  successions of the left elements, respectively. Stable spatially asymmetric solutions with  $x_n < 0$  ( $1 \leq n < n_0$ ),  $x_{n_0} = 0$  ( $2 \leq n_0 \leq N - 1$ ,  $n_0 \neq N/2$ ), and  $x_n > 0$  ( $n_0 < n \leq N$ ) are also generated through saddle-node bifurcations when  $N \geq 4$ . The values of  $g$  at the saddle-node bifurcations depend on the number of negative neurons ( $n_0 - 1$ ) for  $n_0 < N/2$  and are the same

as those with the width  $2(n_0 - 1)$  of a smaller bump in a ring of neurons, e.g.,  $g_{SN} = 3.88$  when the bump width is two ( $n_0 = 2$ ).

When coupling is symmetric [Eq. (2)], metastable dynamical transient patterns exist in the same manner as a ring of neurons. The duration of spatially asymmetric patterns with the initial width  $l_0$  ( $< N/2$ ) of a smaller bump in a chain of  $N$  neurons under the initial condition given in Eq. (13) and a Dirichlet (Neumann) boundary condition is almost (exactly) the same as that of spatially asymmetric patterns with the initial width  $l_0 + 1$  ( $2l_0$ ) in a ring of  $2(N + 1)$  ( $2N$ ) neurons. When coupling is asymmetric [ $d \neq 0$  in Eq. (20)], no traveling wave solutions exist under both boundary conditions when  $N$  is finite and then metastable dynamical transient propagating waves disappear. Spatially nonuniform steady solutions generated from the origin through pitchfork bifurcations are never stabilized as  $g$  increases. The branches of the pitchfork bifurcation for  $d = 0$  break up into a branch without bifurcations and a pair of saddle-node bifurcation branches when  $d \neq 0$ . The stable spatially nonuniform solution is generated through the saddle-node bifurcation. There are no symmetric solutions in which the eigenvalues of the Jacobian matrix exponentially decrease with  $N$ , and thus metastable dynamical transient patterns do not emerge.

- 
- [1] K. Kawasaki and T. Ohta, *Physica A* **116**, 573 (1982); J. Carr and R. L. Pego, *Commun. Pure Appl. Math.* **42**, 523 (1989); G. Fusco and J. K. Hale, *J. Dynam. Differ. Equ.* **1**, 75 (1989); L. Bronsard and R. V. Kohn, *Commun. Pure Appl. Math.* **43**, 983 (1990); S.-I. Ei and T. Ohta, *Phys. Rev. E* **50**, 4672 (1994).
- [2] M. J. Ward, *SIAM J. Appl. Math.* **56**, 1247 (1996); *Boundaries, Interfaces, and Transitions*, CRM Proceedings and Lecture Notes, edited by M. C. Delfour (American Mathematical Society, Providence, 1998), Vol. 13, p. 237; in *Multiple Time-Scale Dynamical Systems*, IMA Volumes in Mathematics and its Applications, edited by C. K. R. T. Jones and A. I. Khibnik (Springer, New York, 2001), Vol. 122, p. 233, references therein.
- [3] D. Estep, *Nonlinearity* **7**, 1445 (1994); C. P. Grant and E. S. Van Vleck, *ibid.* **8**, 861 (1995); S.-N. Chow, J. Mallet-Paret, and E. S. Van Vleck, in *Discretely-Coupled Dynamical Systems*, edited by V. Perez-Munuzuri, L. O. Chua, V. Perez-Villar, and M. Markus (World Scientific, Singapore, 1997), p. 17.
- [4] C. M. Elliott and A. M. Stuart, *SIAM J. Numer. Anal.* **30**, 1622 (1993); J. K. Hale, in *Chaotic Numerics*, edited by P. E. Kloeden and K. J. Palmer (American Mathematical Society, Providence, RI, 1994), Vol. 172, p. 1; L. Nizhnik, L. Nizhnik, and M. Hasler, *Int. J. Bifurcation Chaos* **12**, 261 (2002).
- [5] J. A. S. Kelso, *Dynamic Patterns: The Self-Organization of Brain and Behavior* (MIT Press, Cambridge, MA, 1995); K. J. Friston, *Neuroimage* **5**, 164 (1997); *Neuroscientist* **7**, 406 (2001); A. A. Fingelkurts and A. A. Fingelkurts, *Int. J. Neurosci.* **114**, 843 (2004); M. I. Rabinovich, P. Varona, A. I. Selverston, and H. D. I. Abarbanel, *Rev. Mod. Phys.* **78**, 1213 (2006); G. Werner, *Bio Systems* **90**, 496 (2007); M. Rabinovich, R. Huerta, and G. Laurent, *Science* **321**, 48 (2008).
- [6] W. J. Freeman, *Biol. Cybern.* **56**, 139 (1987); C. A. Skarda and W. J. Freeman, *Behav. Brain Sci.* **10**, 161 (1987).
- [7] I. Tsuda, *World Futures* **32**, 167 (1991); *Behav. Brain Sci.* **24**, 793 (2001); *Chaos* **19**, 015113 (2009).
- [8] M. Rabinovich, A. Volkovskii, P. Lecanda, R. Huerta, H. D. I. Abarbanel, and G. Laurent, *Phys. Rev. Lett.* **87**, 068102 (2001); V. I. Nekorkin, D. V. Kasatkin, and A. S. Dmitrichev, *Radiophys. Quantum Electron.* **53**, 45 (2010); M. A. Komarov, G. V. Osipov, and J. A. K. Suykens, *Europhys. Lett.* **91**, 20006 (2010).
- [9] A. Zumdieck, M. Timme, T. Geisel, and F. Wolf, *Phys. Rev. Lett.* **93**, 244103 (2004).
- [10] R. Zillmer, R. Livi, A. Politi, and A. Torcini, *Phys. Rev. E* **74**, 036203 (2006); *Neurocomputing* **70**, 1960 (2007); S. Jahnke, R. M. Memmesheimer, and M. Timme, *Phys. Rev. Lett.* **100**, 048102 (2008); R. Zillmer, N. Brunel, and D. Hansel, *Phys. Rev. E* **79**, 031909 (2009).
- [11] B. Cessac, *J. Math. Biol.* **56**, 311 (2008); B. Cessac and T. Viéville, *Front. Comput. Neurosci.* **2**, 2 (2008).
- [12] A. Kumar and S. Schrader, *Neural Comput.* **20**, 1 (2008); S. El Boustani and A. Destexhe, *ibid.* **21**, 46 (2009); A. Destexhe, *J. Comput. Neurosci.* **27**, 493 (2009).
- [13] Y. Horikawa and H. Kitajima, *Chaos* **22**, 033115 (2012).
- [14] U. Bastolla and G. Parisi, *J. Phys. A* **31**, 4583 (1998).
- [15] E. Goles and S. Martinez, *Complex Systems* **3**, 589 (1989); R. Ndoundama and M. Tchuenteb, *Theor. Comput. Sci.* **306**, 513 (2003).
- [16] J. Šíma and P. Orponen, *Theor. Comput. Sci.* **306**, 353 (2003).
- [17] Y. Horikawa and H. Kitajima, *Physica D* **238**, 216 (2009).
- [18] Y. Horikawa and H. Kitajima, *Phys. Rev. E* **80**, 021934 (2009).
- [19] S. Amari, *IEEE Trans. SMC-2*, 643 (1972); H. R. Wilson and J. D. Cowan, *Biophys. J.* **12**, 1 (1972); S. Grossberg, *Stud. Appl. Math.* **52**, 213 (1973).
- [20] J. J. Hopfield, *Proc. Natl. Acad. Sci. U.S.A.* **81**, 3088 (1984).

- [21] L. Chua and L. Yang, *IEEE Trans. Circuits Syst.* **35**, 1257 (1988); P. Thiran, *Dynamics and Self-Organization of Locally Coupled Neural Networks* (Presses Polytechniques et Universitaires Romandes, Lausanne, 1997).
- [22] P. Thiran, K. R. Crouse, L. O. Chua, and M. Hasler, *IEEE Trans. Circuits Syst. I* **42**, 757 (1995).
- [23] S. A. Campbell, in *Differential Equations with Applications to Biology*, edited by S. Ruan, Gail S. K. Wolkowicz, and J. Wu (American Mathematical Society, Providence, RI, 1998), p. 65; S. A. Campbell, Y. Yuan, and S. D. Bungay, *Nonlinearity* **18**, 2827 (2005); S. Guo and L. Huang, *Acta Math. Sin.* **23**, 799 (2007); X. Xu, *J. Phys. A* **41**, 035102 (2008).
- [24] K. L. Babcock and R. M. Westervelt, *Physica D* **28**, 305 (1987); P. Baldi and A. F. Atiya, *IEEE Trans. Neural Netw.* **5**, 612 (1994); K. Pakdaman, C. P. Malta, C. Grotta-Ragazzo, O. Arino, and J.-F. Vibert, *Phys. Rev. E* **55**, 3234 (1997).
- [25] Y. Horikawa, *J. Theor. Biol.* **289**, 151 (2011).
- [26] P. S. Churchland and T. J. Sejnowski, *The Computational Brain* (MIT Press, Cambridge, 1992); G. M. Shepherd, *Neurobiology*, 2nd ed. (Oxford University Press, New York, 1988).
- [27] E. Bushong, M. E. Martone, Y. Z. Jones, and M. H. Ellisman, *J. Neurosci.* **22**, 183 (2002); M. M. Halassa, T. Fellin, H. Takano, J. H. Dong, and P. G. Haydon, *ibid.* **27**, 6473 (2007); J. J. Wade, L. J. McDaid, J. Harkin, V. Crunelli, and J. A. Scott Kelso, *PLoS ONE* **6**, e29445 (2011).
- [28] U. Kling and G. Székely, *Kybernetik* **5**, 89 (1968); W. O. Friesen and G. S. Stent, *Biol Cybern* **28**, 27 (1977); *Annu. Rev. Biophys. Bioeng.* **7**, 37 (1978).
- [29] M. Golubitsky, I. Stewart, and D. G. Schaeffer, *Singularities and Groups in Bifurcation Theory II* (Springer, New York, 1988); J. J. Collins and I. Stewart, *Biol. Cybern.* **71**, 95 (1994).
- [30] E. J. Doedel, *AUTO: Software for Continuation and Bifurcation Problems in Ordinary Differential Equations*, Concordia University, Montreal, Canada, <http://indy.cs.concordia.ca/auto/>.
- [31] F. Schlögl, C. Escher, and R. S. Berry, *Phys. Rev. A* **27**, 2698 (1983); A. VI. Gurevich, S. L. Leikin, and R. G. Mints, *Phys. Lett. A* **105**, 31 (1984); A. Engel, *ibid.* **113**, 139 (1985).
- [32] J. Bell, *Math. Biosci.* **54**, 181 (1981); J. P. Keener, *SIAM J. Appl. Math.* **47**, 556 (1987); *J. Theor. Biol.* **148**, 49 (1991); V. Booth and T. Erneux, *Physica A* **188**, 206 (1992); J.-P. Laplante and T. Erneux, *J. Phys. Chem.* **96**, 4931 (1992).
- [33] Y. Horikawa, *Phys. Rev. E* **78**, 066108 (2008).
- [34] A. L. Hodgkin, *J. Physiol.* **107**, 165 (1948); J. A. Connor, D. Walter, and R. Mckown, *Biophys. J.* **18**, 81 (1977); J. Rinzel and G. B. Ermentrout, in *Methods in Neuronal Modeling*, edited by C. Koch and I. Segev (MIT Press, Cambridge, MA, 1989), p. 135; B. Ermentrout, *Neural Comput.* **8**, 979 (1996); E. M. Izhikevich, *IEEE Trans. Neural Netw.* **10**, 499 (1999).
- [35] C. Morris and H. Lecar, *Biophys. J.* **35**, 193 (1981).
- [36] J. L. Hindmarsh and R. M. Rose, *Proc. R. Soc. Lond. B* **221**, 87 (1984); R. M. Rose and J. L. Hindmarsh, *ibid.* **237**, 267 (1989).
- [37] A. N. Burkitt, *Biol. Cybern.* **95**, 1 (2006).
- [38] Y. Horikawa and H. Kitajima, *Physica D* **238**, 2409 (2009); *Neurocomputing* **73**, 3169 (2010).
- [39] Y. Horikawa and H. Kitajima, *Physica D* **241**, 106 (2012).
- [40] Y. Horikawa and H. Kitajima, *Nonlinear Dyn.* **70**, 1079 (2012).